# A comparative analysis of memory B cell and antibody responses against *Plasmodium falciparum* merozoite surface protein 1 in children and adults from Uganda

S. Jake Gonzales[1], Kathleen N. Clarke[1], Gayani Batugedara[1], Ashley E. Braddom[1], Rolando Garza[1], Raphael A. Reyes[1], Isaac Ssewanyana[2,3], Kendra C. Garrison[4], Gregory C. Ippolito[5], Bryan Greenhouse[6], Sebastiaan Bol[1], and Evelien M. Bunnik[1]*

[1] Department of Microbiology, Immunology and Molecular Genetics, Long School of Medicine, The University of Texas Health Science Center at San Antonio, San Antonio, TX, USA

[2] Infectious Disease Research Collaboration, Kampala, Uganda

[3] London School of Hygiene and Tropical Medicine, London, UK

[4] Department of Chemical Engineering, University of Texas at Austin, Austin, TX, USA

[5] Department of Molecular Biosciences and Department of Oncology, Dell Medical School, University of Texas at Austin, Austin, TX 78712, USA

[6] Department of Medicine, University of California San Francisco, San Francisco, CA, USA

***Correspondence**

Evelien M. Bunnik, Ph.D.

bunnik@uthscsa.edu

7703 Floyd Curl Drive

San Antonio, TX 78229

United States of America

**Keywords:** adaptive immune response; humoral immunity; IgM; IgG; somatic hypermutation; antibodies; memory B cells

## Abstract

Memory B cells (MBCs) and plasma antibodies against *Plasmodium falciparum* merozoite antigens are important components of the protective immune response against malaria. To gain understanding of how responses against *P. falciparum* develop in these two arms of the humoral immune system, we evaluated MBC and antibody responses against the most abundant merozoite antigen, merozoite surface protein 1 (MSP1), in individuals from a region in Uganda with high *P. falciparum* transmission. Our results showed that MSP1-specific B cells in adults with immunological protection against malaria were predominantly $IgG^+$ classical MBCs, while children with incomplete protection mainly harbored $IgM^+$ MSP1-specific classical MBCs. In contrast, anti-MSP1 plasma IgM reactivity was minimal in both children and adults. Instead, both groups showed high plasma IgG reactivity against MSP1 and whole merozoites, with broadening of the response against non-3D7 strains in adults. The antibodies encoded by MSP1-specific $IgG^+$ MBCs carried high levels of amino acid substitutions and recognized relatively conserved epitopes on the highly variable MSP1 protein. Proteomics analysis of $MSP1_{19}$-specific IgG in plasma of an adult revealed a limited repertoire of anti-MSP1 antibodies, most of which were $IgG_1$ or $IgG_3$. Similar to MSP1-specific MBCs, anti-MSP1 IgGs had relatively high levels of amino acid substitutions and their sequences were predominantly found in classical MBCs, not atypical MBCs. Collectively, these results showed evolution of the MSP1-specific humoral immune response with cumulative *P. falciparum* exposure, with a shift from $IgM^+$ to $IgG^+$ B cell memory, diversification of B cells from germline, and stronger recognition of MSP1 variants by the plasma IgG repertoire.

## Introduction

Malaria, caused by the parasite *Plasmodium falciparum*, is responsible for approximately half a million deaths every year, of which two-thirds occur in children under the age of five (1). A much larger number of people experience non-fatal malaria, amounting to an estimated 230 million cases of disease annually. Although the mortality rate for malaria has slowly but consistently declined over the past two decades, the decrease in malaria incidence has plateaued in the past five years. Current interventions are thus insufficient for malaria elimination and novel tools, such as a highly efficacious malaria vaccine, are urgently needed in the fight against this devastating disease. RTS,S, the only malaria vaccine that has elicited protection against (severe) malaria in a phase III clinical trial, had an efficacy against clinical malaria of 30 – 40% in infants and young children (2). Vaccine efficacy was high shortly after vaccination but declined rapidly, and was lower against parasites that were genetically different from strain 3D7 that the subunit vaccine RTS,S was based on (3). Compared to vaccination, repeated natural *P. falciparum* infections eventually elicit superior immunity, consisting of relatively long-lived antibody responses (~2 – 4 years) with cross-strain reactivity (4, 5). This naturally acquired humoral immunity against malaria is associated with the presence of circulating immunoglobulin G (IgG) against *Plasmodium* blood stage antigens (6-13). Recently, immunoglobulin M (IgM) has received increased attention as IgM responses were also shown to correlate with protection and were able to inhibit parasite growth *in vitro* (14-16). A complete understanding of the development of humoral immune responses against *P. falciparum*

blood stage antigens over time will help with the development of a more effective and longer lasting vaccine than RTS,S.

Effective and long-lasting humoral immune responses against pathogens consist of long-lived memory B cells (MBCs) in the circulation and plasma cells that reside in the bone marrow and secrete large amounts of antibody into the circulation (reviewed in (17)). In the case of *P. falciparum*, long-lived humoral immunity develops over the course of years of repetitive infections, leaving young children largely susceptible to disease. With cumulative *P. falciparum* exposure, the quality of B cell responses gradually improves. Both MBCs and plasma cells generated in response to *P. falciparum* infection are short-lived in young children but gradually increase in longevity in adolescents and adults (4, 18, 19). Over time, antibody responses also recognize a larger number of parasite antigens (18). In addition, recurrent infections drive the generation of antibodies capable of mediating cross-strain immunity, which is strongly associated with protection (5). Most studies into the development of antibody responses against *P. falciparum* have been performed using serum. However, this prevents investigating the molecular characteristics of *P. falciparum*-specific antibodies. In addition, little is known about the connection between the MBC and plasma cell compartments. This information will be useful for understanding how durable immunity against malaria develops and may enable us to harness lessons from naturally acquired immunity for improved vaccine design.

In this study, we set out to investigate differences in humoral immune responses in between children with incomplete protection against malaria and adults who have developed strong immunological protection to better understand how MBC and antibody

98 responses develop over the course of life-long *P. falciparum* exposure. To do this, we
99 compared the antibody and MBC response against *P. falciparum* antigen merozoite
100 surface protein 1 (MSP1) between children and adults living in a region of high *P.*
101 *falciparum* transmission in Uganda. MSP1 is a large, polymorphic, and highly
102 immunogenic protein expressed ubiquitously on the surface of the parasite during the
103 late schizont and merozoite stages (20, 21). MSP1 has long been considered a vaccine
104 target since antibody responses against this protein have been associated with
105 protection (6, 20, 22), although results from MSP1-based vaccine trials have been
106 disappointing (23, 24). However, since MSP1 has high antigenic heterogeneity across
107 *P. falciparum* strains, we considered it an excellent model antigen to assess antibody
108 cross-strain reactivity elicited by natural infection. We studied the isotype of MSP1-
109 specific MBCs, sequence characteristics of monoclonal antibodies isolated from $IgM^+$
110 and $IgG^+$ MBCs, and cross-strain reactivity against MSP1 variants in both plasma
111 antibodies and B cells. In addition, we analyzed the anti-MSP1 plasma IgG repertoire
112 and investigated characteristics of antibodies that were found in both the MBC and
113 plasma IgG compartment in more detail.

114

115 **Results**

116 **MSP1-specific B cells have a classical phenotype and are enriched for IgG in**
117 **adults**

118 To study differences in naturally acquired B cell responses against MSP1 between
119 partially immune and immune individuals, we selected four children and four adults
120 residing in Tororo, Uganda, a region with high malaria transmission intensity year-round

(**Supplementary table 1**) (25). These individuals were participants of cohort studies, with the exception of two Ugandan adults who were anonymous blood donors with high levels of plasma antibodies against various malaria antigens, suggesting frequent exposure to *P. falciparum* (**Supplementary figure 1**). Cryopreserved PBMCs were used to first isolate bulk B cells, followed by staining with fluorescently labeled tetramers of full-length MSP1 from *P. falciparum* strain 3D7 ($MSP1_{3D7}$) and decoy tetramers for analysis by flow cytometry, a strategy developed and used by others (26, 27) (**Figure 1A**). In both children and adults, MSP1-specific B cells (defined as $CD19^+CD20^+MSP1^+decoy^-$) were predominantly found among $CD21^+CD27^+$ classical memory B cells (MBCs) (**Figure 1B**). In addition, in both groups, very few MSP1-specific B cells were found among $CD21^-CD27^-$ atypical MBCs (**Figure 1B**). To further define the phenotype of MSP1-specific B cells, we determined the isotype usage of MSP1-specific classical MBCs. Children showed much larger percentages of $IgM^+$ (median, ~70%) than $IgG^+$ (median, ~10%) classical MBCs in the total repertoire, which was reflected in the percentage of $IgM^+$ and $IgG^+$ MSP1-specific classical MBCs (**Figure 1C**). In contrast, $IgM^+$ and $IgG^+$ classical MBCs were equally abundant in adults in the total repertoire, while $IgM^+$ MSP1-specific classical MBCs were depleted and $IgG^+$ MSP1-specific classical MBCs were slightly enriched (**Figure 1C**). The ratio of $IgG^+$ to $IgM^+$ MSP1-specific classical MBCs was higher in all adults as compared to the children (**Figure 1D**). Collectively, these results suggest that the B cell response against MSP1 is skewed to $IgM^+$ classical MBCs in children, while it is dominated by $IgG^+$ classical MBCs in adults. These results are in line with a recent report that showed an increased frequency of IgM usage among *P. falciparum*-specific B cells in young children as

compared to older children and adults in Mali, where malaria transmission is highly seasonal (16), suggesting that this is a general feature of the B cell response to *P. falciparum* in children in malaria-endemic regions.

## Recombinant antibodies from isolated memory B cells are MSP1-specific and inhibit parasite growth

To confirm antigen-specificity of MSP1-specific B cells, all $IgM^+$ and $IgG^+$ MSP1-specific B cells were single-cell-sorted into 96-well culture plates containing CD40L-expressing feeder cells, cytokines, and other stimuli that collectively promote B cell survival, expansion, and differentiation into antibody-secreting cells. This allowed us to screen B cell clones for antigen-specificity prior to cloning and expression of recombinant mAbs. B cell supernatants were tested for the presence of anti-MSP1 antibodies by a *P. falciparum* strain 3D7 merozoite ELISA or Luminex assay using recombinant $MSP1_{3D7}$. These assays were implemented into our analysis pipeline only in later experiments and these data are therefore missing for samples analyzed earlier. The variable regions of antibodies with confirmed reactivity to merozoites or recombinant MSP1 were cloned into linear expression cassettes, expressed as recombinant $IgG_1$, and against tested for MSP1 reactivity (**Figure 2A**). As was reported in a recently published article (15), most anti-MSP1 IgM antibodies lost their reactivity to MSP1 when expressed as $IgG_1$, which is likely a result of the lower avidity of monomeric IgG as compared to pentameric IgM. We therefore cloned a multimerization domain into the C-terminus of the $IgG_1$ heavy chain to express IgM-derived antibodies as pentameric IgG. In contrast to results reported by Thouvenel *et al*. (15), we were unable to rescue the MSP1-reactivity of IgM-

167 derived variable regions by expression as pentameric IgG (**Figure 2A**). The only
168 pentameric IgG with reactivity to MSP1 was also reactive when expressed in
169 monomeric form. To further confirm the specificity and functionality of the isolated anti-
170 MSP1 mAbs, we performed immunofluorescence assays on segmented schizonts for
171 three randomly selected IgG mAbs, showing the expected surface staining of
172 merozoites (**Figure 2B**). We also performed growth-inhibition assays for six IgG mAbs
173 that were selected based on high expression levels in culture. At a concentration of 200
174 µg/ml, these six mAbs showed on average 51% (range, 17% – 65%) inhibition of *P.*
175 *falciparum* growth as compared to a negative control, demonstrating their ability to
176 functionally inhibit the parasite (**Figure 2C**).

177

178 **MSP1-specific IgG$^+$ MBC lineages from a malaria-experienced adult are highly**
179 **diversified and expanded**

180 Next, we set out to study the molecular characteristics of antibodies encoded by MSP1-
181 specific MBCs. In total, we isolated 6 IgM and 25 IgG mAbs with confirmed MSP1
182 reactivity from 6 donors. Full-length heavy and light chain variable regions were
183 obtained and analyzed using IMGT/V-QUEST (28) to determine the level of amino acid
184 substitutions in the V gene segments of the variable regions. MSP1-specific IgM$^+$ MBCs
185 from adults and children carried few amino acid substitutions in both the heavy and light
186 chain V gene segments (average, <1% amino acid changes), while many of the IgG$^+$
187 MBCs were highly mutated (>15% amino acid changes; **Figure 3A,B**). None of the IgM$^+$
188 MBCs were clonally related to each other, defined as sequences using the same heavy
189 chain V and J gene and having a highly similar heavy chain complementarity

determining region 3 (HCDR3; ≥85% amino acid similarity). In contrast, several clonally expanded IgG$^+$ MBC lineages were identified in adult donor 2, from whom most mAbs were derived (**Figure 3A,B**). B cells belonging to expanded lineages were among those that were the most diversified from the germline antibody sequences, particularly in the heavy chain V gene segment. Finally, although there was no statistically significant difference in the length of the HCDR3 between IgM and IgG sequences, several IgG sequences harbored long HCDR3s (≥20 amino acids), while IgM sequences had average or relatively short HCDR3s (**Figure 3C**).

## Anti-MSP1 plasma antibody responses are dominated by IgG in both children and adults

A study of B cell responses upon influenza virus vaccination reported that the largest clonal B cell families were directed against the most conserved epitopes (29). Based on these observations, we hypothesized that clonally expanded anti-MSP1 IgG$^+$ MBC lineages would have cross-strain reactivity, whereas non-expanded IgG$^+$ MBC lineages would be strain-specific. To test this hypothesis, we developed a Luminex assay using beads coated with full-length MSP1 variants from the geographically and genetically distinct *P. falciparum* strains 3D7 (African origin), Dd2 (South-east Asian origin), and HB3 (Central American origin). 21 out of 22 mAbs (95%) tested in this assay bound to $MSP1_{3D7}$ (**Figure 4A**). This high reactivity with $MSP1_{3D7}$ was expected since $MSP1_{3D7}$ was used for the isolation of MSP1-specific B cells. It is therefore unclear why one mAb bound $MSP1_{Dd2}$ but not $MSP1_{3D7}$. All other mAbs showed reactivity with at least one other MSP1 variant, and the majority showed reactivity with both $MSP1_{Dd2}$ and

213 $MSP1_{HB3}$, including all mAbs from the largest clonal lineage (**Figure 4A**). These results
214 suggest that the majority mAbs recognized relatively conserved epitopes, irrespective of
215 the level of clonal expansion of the B cell lineage. Unfortunately, we were unable to
216 determine reactivity of mAbs isolated from $IgM^+$ MBCs against the three MSP1 variants
217 from different *P. falciparum* strains, because of the loss of antigen reactivity when these
218 mAbs were expressed as IgG. In addition, most mAbs were derived from a single donor,
219 limiting the conclusions we could draw from this experiment.

220

221 To expand on the results of cross-strain reactivity of mAb against MSP1 and to
222 determine whether the MSP1-specific MBC isotype differences we observed between
223 children and adults are reflected in the plasma antibody response, we tested plasma
224 samples from 24 adults and 18 children for IgM and IgG reactivity against MSP1 from
225 the three *P. falciparum* strains (**Supplementary table 2**). This experimental design
226 provides a measurement of the overall antibody reactivity of the plasma but does not
227 discriminate between antibodies with cross-strain reactivity or a combination of multiple
228 strain-specific antibodies. However, it will reveal whether anti-MSP1 antibody responses
229 broaden with cumulative *P. falciparum* exposure. As a control, we included plasma
230 samples from recovered US COVID-19 patients who showed IgM and IgG reactivity
231 against the SARS-CoV-2 receptor binding domain, but not against the three *P.*
232 *falciparum* MSP1 variants. In both children and adults, anti-MSP1 IgM reactivity in the
233 plasma was very low, although four of the 24 adult samples contained anti-MSP1 IgM
234 against at least one MSP1 variant antigen (**Figure 4B**). In contrast, all samples showed
235 strong IgG reactivity against all MSP1 variants (**Figure 4C**). Adults had higher plasma

IgG reactivity against $MSP1_{HB3}$ than children. The average reactivity of adult samples against $MSP1_{Dd2}$ was also higher but not statistically significantly different from that in children (P = 0.06). These results suggest that while children already have plasma IgG against different variants of MSP1, this response continues to broaden with age.

To determine whether the differential IgM and IgG reactivity of plasma is specific for anti-MSP1 antibodies or can be extrapolated to anti-merozoite antibody responses in general, we also tested reactivity of plasma IgM and IgG to whole merozoites from *P. falciparum* strain 3D7. In this assay, we observed anti-IgM and anti-IgG reactivity in both groups, with adults showing higher reactivity for both IgM and IgG as compared to children (**Figure 4D**). IgM and IgG anti-merozoite reactivity were not directly compared since the values measured could have been influenced by the binding affinity of the secondary antibody. Collectively, these results suggest that in contrast to our observation that the MBC response in children is enriched for $IgM^+$ MBCs, the plasma antibody response against MSP1 in both children and adults is dominated by IgG. However, IgM responses against other merozoite antigens may be better developed, in particular in adults.

**The anti-MSP1 plasma IgG repertoire has limited diversity, high levels of amino acid substitutions, and mainly overlaps with sequences found in classical memory B cells**

To further explore the connection between the plasma cell and MBC compartments of the humoral immune response, we performed an integrative analysis of the plasma anti-MSP1 IgG and B cell receptor repertoires in adult donor 2, who was selected based on

the availability of additional PBMCs and plasma. Although the results of this experiment will require confirmation in additional individuals, this is the first analysis of its kind in a malaria-experienced person and will provide valuable insight into the molecular characteristics of the anti-MSP1 plasma antibody repertoire after life-long exposure to *P. falciparum*. In a previous study, we generated B cell receptor sequencing (BCR-seq) data of antibody heavy chain variable regions of naïve B cells, classical MBCs, and atypical MBCs (30). The full BCR-seq data set and all sequences obtained from MSP1-specific MBCs were used to construct a personalized, donor-specific reference heavy chain antibody variable region sequence database. We then isolated anti-MSP1 IgG from plasma using commercially available 19 kDa C-terminal fragment of MSP1 ($MSP1_{19}$), which limited our analysis to the most conserved domain of MSP1 (31, 32). We analyzed the anti-$MSP1_{19}$ IgG preparation by high-resolution liquid chromatography with tandem mass spectrometry and searched the obtained spectra against the donor-specific antibody variable region database (**Figure 5A**). This step allowed us to identify the full-length antibody sequences that these short peptide spectra were derived from. Eighteen anti-$MSP1_{19}$ IgG lineages were identified, of which four lineages made up over 75% of all plasma anti-$MSP1_{19}$ IgG (**Figure 5B, Supplementary table 3**), suggesting that the anti-MSP1 plasma IgG repertoire is relatively limited in diversity. The 18 antibody lineages were dominated by sequences that were found among $IgG_1^+$ and $IgG_3^+$ classical MBCs, all of which had relatively high levels of amino acid substitutions (>15%) (**Figure 5B**). These results suggest that MSP1-specific B cell lineages can give rise to both plasma cells and classical memory B cells, but not atypical MBCs. Two relatively abundant antibody lineages (comprising 23.5% and 6.9% of anti-$MSP1_{19}$

plasma IgG) overlapped with $IgG^+$ classical MBC lineages that were expanded in the bulk BCR-seq data (5 and 4 clonal B cell members, respectively). Both of these lineages used IGHV1-69 and IGHJ6 and had long HCDR3 sequences of 24 and 21 amino acid residues, respectively, suggesting that these characteristics may have contributed to the selection and expansion of both MBC and plasma cell populations. Long HCDR3s were also observed among the other IgG clonal lineages (average of all lineages, 18 amino acid residues; **Supplementary table 3**), although the most abundant IgG (representing 24.7% of all anti-$MSP1_{19}$ plasma IgG) had an HCDR3 of 10 amino acid residues. A third antibody lineage with low abundance (<0.1%) matched with an expanded B cell lineage, consisting of two clonal $IgM^+$ atypical MBC members that had relatively high levels of amino acid substitutions (>10%). Except for these three expanded lineages, all other clonotypes were found as a single sequence in the bulk BCR-seq data set. These results highlight that the abundance of antibody clonotypes in the plasma is not necessarily reflected by an expansion of the corresponding MBC lineages, pointing towards different selective mechanisms that govern MBC and plasma cell development.

## Analysis of an expanded B cell lineage detected in both plasma IgG and memory B cells

To further analyze antibody characteristics that may influence their selection and expansion among plasma cells and MBCs, we compared the anti-MSP1 IgG sequences detected in plasma with those derived from MSP1-specific MBCs. Only the largest MSP1-specific mAb lineage was detected among the anti-$MSP1_{19}$ antibody lineages

identified in plasma, potentially because other MSP1-specific mAbs target epitopes in other parts of the MSP1 protein. Two mAb sequences of this clonal lineage, mAb10 and mAb22, were found in plasma at a percentage of 6.8% and 0.1% of all anti-MSP1 IgG detected, respectively, making it the fifth largest clonotype in the circulation. Despite having highly similar heavy chain variable regions, including eight shared amino acid substitutions and a long HCDR3 sequence (21 amino acid residues, **Supplementary figure 2**), mAb10 and mAb22 had different light chains. Like all other members of the clonal lineage (total n = 9), mAb22 had a lambda light chain, while mAb10 contained a kappa light chain. mAb10 was more abundant in plasma (6.8%), but was the only member of the MBC lineage with a kappa light chain. The opposite was observed for the lambda light chain variants, found at 0.1% of all anti-MSP1 plasma IgG, but representing eight out of nine members of the MSP1-specific MBC lineage. This difference in relative abundance of lineage members in different B cell compartments may be related to the preferential differentiation of high-affinity B cells to plasma cells and lower-affinity B cells to MBCs (33). For mAb10 and mAb22, it would therefore be expected that mAb10 has higher antigen-binding affinity. We determined binding affinity of mAb10 and mAb22 to MSP1 using a chaotropic ELISA with urea and observed that mAb10 indeed showed higher binding affinity to MSP1 than mAb22 (**Figure 6A**). The observation that mAb10 and mAb22 had different light chains suggests that antigen binding by these mAbs is dominated by their heavy chain. To test this, we expressed mAb22 with light chains from unrelated non-MSP1-binding antibodies and observed that it was still reactive with $MSP1_{3D7}$, albeit with lower binding affinity (**Figure 6B**). These results suggest that the heavy chain of mAb22 (and presumably mAb10) is sufficient for

binding to MSP1, but that its light chain is important for optimal binding to antigen. This raised the question whether the difference in binding affinity between mAb10 and mAb22 is caused by the different light chains used by the two mAbs. For each mAb, we therefore compared binding affinity between the antibody expressed with its own light chain and a chimeric antibody in which the light chain was swapped. Expression of mAb10 with the mAb22 light chain resulted in a reduction of binding affinity, while the binding affinity of mAb22 was unchanged when expressed with the mAb10 light chain (**Figure 6C**). These results suggest that the light chain of mAb10 may play a role in the increased binding affinity of mAb10 over mAb22, but is dependent on the mAb10 heavy chain for this effect. Interestingly, despite higher binding affinity, mAb10 showed reduced activity in a growth inhibition assay as compared to mAb22 (**Figure 2C**). Collectively, these results highlight characteristics of the individual members of an MSP1-specific clonal B cell lineage that may have influenced their selection and fate.

## Discussion

The prevalence and magnitude of antibody responses against *P. falciparum* merozoite antigens have been extensively studied. However, much remains unknown about the molecular characteristics of anti-merozoite antibodies and the connections between the MBC and plasma cell compartments. This information will increase our understanding of how durable B cell immunity develops and how this may be harnessed for vaccine development. Here, we compared the phenotype and molecular characteristics of MBCs against the most abundant merozoite surface antigen, MSP1, between children and adults living in a region of high *P. falciparum* transmission in Uganda. In addition, we

351 analyzed cross-strain reactivity among anti-MSP1 plasma IgM and IgG in both children
352 and adults. Finally, we analyzed the overlap between the MBC and plasma antibody
353 compartments in detail for one adult to better understand the processes that drive B cell
354 selection and fate decisions.

355

356 Our results showed that children harbored a larger fraction of MSP1-specific $IgM^+$ MBCs
357 than adults, in line with a recent report (16). Interestingly, based on these observations,
358 one might expect that the plasma anti-MSP1 antibody response would also be
359 dominated by IgM, but this was not the case. In both adults and children, the level of
360 anti-MSP1 in plasma was much lower than that of anti-MSP1 IgG. We recognize that it
361 is difficult to directly compare IgM and IgG measurements due to potential differences
362 between secondary antibodies used in these assays. However, our control samples
363 from recovered COVID-19 patients demonstrate that we were able to measure IgM
364 reactivity, yet we detected plasma IgM reactivity against MSP1 in only a small
365 percentage of adults. These observations suggest that malaria-experienced children
366 develop a strong IgG response against MSP1 that is not reflected in the MBC
367 compartment. One explanation for the relative lack of $IgG^+$ MBCs in children could be
368 that the B cell response predominantly gives rise to short-lived $IgG^+$ plasmablasts,
369 whereas germinal center reactions are limited. Since germinal center responses are
370 essential for the development of long-lived plasma cells and MBCs, this would explain
371 the relatively quick waning of anti-parasite plasma IgG and MBCs in children in the
372 absence of exposure, as seen in children living in malaria-endemic regions with a
373 distinct dry season (18, 19). It has been shown that *P. falciparum* infections can lead to

dysregulation of various components of the immune system that are essential for the formation of germinal centers, including dendritic cells and T follicular helper cells (34-37). In addition, the abundant development of plasmablasts during *Plasmodium* infection in rodents directly limited the generation of germinal centers as a result of nutrient depletion (38). In this scenario, $IgM^+$ MBCs would mainly develop outside of germinal centers, which would be in agreement with the low levels of somatic hypermutation that we observed. An alternative explanation for our observation could be that anti-merozoite $IgG^+$ MBCs are formed equally efficiently in both children and adults but undergo recall shortly after their formation in children as a result of repetitive *P. falciparum* infections with high parasitemia, whereas the lower antigenic load of asymptomatic infections in adults would allow for a longer lifespan of $IgG^+$ MBCs. This theory would be in line with the increase in the percentage of merozoite-specific MBCs with age that is observed in individuals who live in malaria-endemic regions (19). In support of this theory is our observation that the few $IgG^+$ MBCs isolated from children already had relatively high levels of amino acid substitutions, suggestive of multiple rounds of affinity maturation in germinal centers. It is also supported by our observation of a lack of clonal connections between $IgG^+$ MBCs at two time points six months apart in two five-year old children living in a high transmission region in Uganda, while we did find clonally related sequences among $IgM^+$ MBCs between the same two time points (Gonzales *et al.*, in press). These data could suggest that the $IgG^+$ MBC compartment in children undergoes more rapid turnover than the $IgM^+$ MBC compartment, or that the $IgM^+$ MBC compartment has more self-renewing capacity (39). It is difficult to untangle various potential scenarios of how B cell responses develop and are influenced by the

chronic and repetitive nature of *P. falciparum* infections. More longitudinal studies in the same individuals will be needed to track the fate of parasite-specific $IgG^+$ MBCs after their formation.

We observed a low level of plasma IgM against both MSP1 and whole merozoites as compared to plasma IgG. This raises the question of how much IgM contributes to the control of *P. falciparum* infections. IgM responses against a variety of *P. falciparum* antigens have been reported in several studies, in particular in high transmission regions (40-43), but there is conflicting evidence on the durability of the IgM response and its role in parasite inhibition. Boyle *et al.* reported that IgM responses against MSP2 were sustained in children living in Kenya during a period with low parasite transmission (14). In contrast, Walker *et al.* concluded that IgM responses against five other merozoite antigens decreased rapidly following *P. falciparum* malaria in children living in Ghana, whereas IgG responses against these five antigens were maintained for a longer period of time (43). These conflicting observations may be the result of differences between the assays used to assess these antibody responses, or differences in the development of IgM responses under different transmission intensities or against different parasite antigens. An association between IgM reactivity against *P. falciparum* antigens, including $MSP1_{19}$, AMA1, MSP3, and GLURP, and protection against malaria was reported by some (14, 44, 45), but not by others (46). When tested at the same concentration, purified plasma IgM from malaria-experienced individuals had equal opsonic phagocytosis activity and two-fold lower fixation capacity of C1q, the primary component of the classical complement pathway, as compared to plasma IgG,

but induced nine-fold higher deposition of components of the membrane attack complex (14, 16). While these results suggest that IgM can indeed contribute to parasite inhibition, the concentration of IgM in plasma is almost one order of magnitude lower than that of IgG (average, 1.5 g/l for IgM versus 11 g/l for IgG, (47, 48)). Therefore, the relative contributions of IgM and IgG to parasite inhibition remain to be determined. Finally, a passive immunization study showed that IgG-depleted plasma from malaria-experienced adults had no effect on parasitemia in children with *P. falciparum* malaria, whereas treatment with IgG from the same individuals resulted in a dramatic decrease of parasite counts (49), suggesting that IgG is the main effector antibody responsible for parasite control.

The acquisition of high levels of amino acid substitutions in $IgG^+$ MBCs from both children and adults suggests that these cells are the product of multiple rounds of affinity selection. We also detected several B cells with long HCDR3s, similar to broadly neutralizing antibodies against HIV (50), although this was not a universal characteristic of anti-MSP1 mAbs. In addition, we observed that children and adults had equally high IgG reactivity against MSP1 3D7, but that reactivity against MSP1 HB3 was lower in children. This suggests that the IgG response continues to broaden with subsequent *P. falciparum* infections, resulting in a larger fraction of IgG directed against conserved epitopes. The broadening of antibody responses, high mutational load, and expansion of clonal MSP1-specific B cell lineages is suggestive of strong selection pressure on the B cell response as a result of *P. falciparum* infections. We believe that our observations regarding mAb10 and mAb22, two members of an MSP1-specific $IgG^+$ MBC lineage

that share the same heavy chain but have different light chains, are additional evidence of strong forces on B cell selection and development. The difference in light chain usage between mAb10 and mAb22 raises the question how these mAbs are developmentally related. One possibility is that mAb10 and mAb22 were derived from a B cell precursor that underwent cell division upon heavy chain rearrangement in the bone marrow, giving rise to multiple daughter cells that each underwent light chain rearrangement independently. In this scenario, the shared amino acid mutations would be the result of convergent evolution selecting for higher affinity antigen binding. In a second scenario, a precursor B cell activated by antigen could have undergone secondary light chain rearrangement in the germinal center. In this case, the kappa light chain-bearing mAb10 would likely be evolutionarily closer to this precursor, and mAb22 (and all other MBCs in this lineage) would be derived from this secondary rearrangement event and have undergone further diversifying selection. We were unable to determine whether mAb10 and mAb22 developed as a result of convergent evolution or clonal lineage diversification. However, our results suggest that the light chains of these antibodies may affect antibody binding affinity. This could, on its own, have resulted in the preferential differentiation of the higher affinity mAb10 variant into a plasma cell and the lower affinity mAb22 variant into an MBC. Further studies into the relationship between the plasma cell and MBC compartments for MSP1 and other merozoite antigens are currently ongoing in our laboratories.

In conclusion, we performed an analysis of the MBC compartment and antibody responses against MSP1 in children and adults living under high *P. falciparum*

466 transmission conditions. We observed that children predominantly harbor MSP1-specific
467 $IgM^+$ MBCs, while the MBC response had shifted to $IgG^+$ B cells in adults. In contrast to
468 this difference in isotype among MSP1-specific MBCs, both children and adults
469 demonstrated strong anti-MSP1 plasma IgG responses, while anti-MSP1 plasma IgM
470 responses were minimal. $IgG^+$ MBCs carried high levels of somatic hypermutations and
471 clonal expansion, suggestive of ongoing B cell selection over the course of sequential
472 *P. falciparum* infections. Finally, we directly compared the overlap between the MSP1-
473 specific MBC compartment and anti-MSP1 plasma IgG, revealing that the same
474 molecular characteristics observed in the MBC compartment were also dominant in the
475 plasma IgG compartment. Collectively, our results provide new insights into the
476 development of B cell responses against *P. falciparum*, in particular about the
477 similarities and differences between MBC and antibody responses.

478

479 **Materials and methods**

480 **Ethics approval statement**

481 Participants were enrolled in the Tororo Child Cohort or the Program for Resistance,
482 Immunology, Surveillance, and Modeling of Malaria (PRISM) Cohort, and provided
483 written consent for the use of their samples for research. These cohort studies were
484 approved by the Makerere University School of Medicine Research and Ethics
485 Committee (SOMREC) and the University of California, San Francisco Human
486 Research Protection Program & IRB. The use of cohort samples was approved by the
487 Institutional Review Board of the University of Texas Health Science Center at San
488 Antonio. Donors 1 and 2 were anonymous blood donors at Mbale regional blood bank in

Eastern Uganda, who consented to the use of their blood for research. The use of samples from anonymous blood donors was considered not human research by the Institutional Review Board of the University of Texas Health Science Center at San Antonio.

COVID-19 samples used in this study were received de-identified from the University of Texas Health San Antonio COVID-19 Repository. This repository was reviewed and approved by the University of Texas Health Science Center at San Antonio Institutional Review Board. All study participants provided written informed consent prior to specimen collection for the repository to include collection of associated clinical information and use of left-over clinical specimens for research. The COVID-19 Repository utilizes an honest broker system to maintain participant confidentiality and release of de-identified data or specimens to recipient investigators.

**Participants**

Malaria-experienced participants were residents of Eastern Uganda, a region with extremely high malaria transmission intensity (annual entomological inoculation rate in the region estimated at 125 infectious bites per person per year (51). In this region, children between five and ten years of age start to develop protective immune responses against malaria but are typically still susceptible to disease. Children above ten years of age and adults have developed protective immune responses, evidenced by no signs of clinical malaria despite high exposure, demonstrated by household

511 entomological and epidemiological measures, including documented asymptomatic
512 parasitemia.

513

514 **MSP1 expression and tetramer synthesis**

515 To produce C-terminal biotinylated 3D7 MSP1, human Expi293F cells (Thermo
516 #A14635) were cultured, passaged, and transfected with the plasmids MSP1-bio
517 (Addgene #47709) and secretedBirA-8his (Addgene #32408) at a 4:1 (w/w) ratio
518 according to Thermo's protocol. Both plasmids were a kind gift from Gavin Wright (52,
519 53). Biotin (Thermo #PI21336) was added to a final concentration of 100 µM
520 immediately after adding the transfection mix. Cell were cultured in either non-baffled
521 polycarbonate flasks with a vent cap (Fisher #PBV12-5) or in glass Erlenmeyer flasks
522 loosely covered with aluminum foil to allow for gas exchange. Cells were successfully
523 passaged in volumes as low as 5 ml. Absence of mycoplasma contamination was
524 confirmed using the MycoAlerta Plus mycoplasma detection kit (Lonza #LT07705).
525 Culture supernatants were collected 5 – 7 days post-transfection by centrifuging the
526 culture at 4,000 × g for 25 min. at RT. A 10 kDa cutoff Protein Concentrator PES
527 (Thermo #88527) was used (5,000 × g at 4ºC) to exchange culture medium containing
528 free biotin for PBS (pH 7.2) (> 100,000 dilution) and to concentrate the protein to a final
529 volume of 0.5 – 1 ml. The 3D7 MSP1 protein was mixed with 6 – 12 volumes of PBS
530 (pH 5.5) in a final volume of six ml and was subsequently loaded onto gravity flow
531 columns (Thermo #29924) containing CaptAvidin agarose (Thermo #C21386) for
532 purification. After three washes with PBS (pH 5.5) and five 6 ml elutions with PBS (pH
533 10.5), the elutions were pooled (30 ml) and the pH was immediately neutralized by

adding 12 ml PBS (pH 5.5). After concentrating, the protein was quantified using the Coomassie Plus (Bradford) Assay Kit (Thermo #23236) on a NanoDrop One spectrophotometer, according to the manufacturer's instructions, visualized by SDS-PAGE (**Supplementary Figure 3A**), diluted to 1 mg/ml, aliquoted, and stored at -70°C.

Since each streptavidin molecule has the ability to bind four biotinylated MSP1 molecules, MSP1 tetramers were made by incubating MSP1 in a tube revolver (Thermo #88881001) at 40 rpm and RT for 30 min. with streptavidin-PE (Thermo #S866) at a 6:1 molar ratio. After this incubation, the tetramers were washed with PBS (pH 7.2) using a Vivaspin centrifugal concentrator (Sartorius #VS0141) three times for 5 min. at 15,000 × g at RT. To make decoy tetramers, streptavidin-PE was first conjugated to Alexa-fluor 647 (Thermo #A20186) per manufacturer's instructions. This double-conjugated streptavidin was then coupled to *R. norvegicus* CD200 (Addgene #36152 (53)) as described above.

**SDS-PAGE**

As a quality control step, purified MSP1 and antibodies were visualized on a polyacrylamide gel. Purified samples were mixed with Laemmli buffer and NuPage sample reducing agent (Thermo #NP0004; not added for monoclonal antibodies), incubated at 85°C for two min. The samples were run on a 4 – 12% Bis-Tris gel (Thermo #NP0321BOX) with MOPS running buffer (Thermo #NP0001) at 200 V for 50

555 min. The proteins were stained using Imperial Coomassie protein stain (Thermo
556 #PI24615) per manufacturer's instructions.

557

558 **MSP1-specific B cells isolations**

559 Cryopreserved peripheral blood mononuclear cells (PBMCs) from malaria-experienced
560 children and adults were thawed in a water bath at 37°C and immediately mixed with
561 pre-warmed thawing medium (IMDM Glutamax (Thermo #31980030) supplemented
562 with 10% heat-inactivated fetal bovine serum (FBS) of US origin (Sigma #TMS-013-B)
563 and 33 U/ml universal nuclease (Thermo #88700)) and then centrifuged (5 min. at 250 ×
564 g and RT). The cell pellet was resuspended in thawing medium and viable cells were
565 counted by adding 10 µl filtered 0.2% trypan blue in PBS to 10 µl of the cell suspension
566 on a Cellometer Mini (Nexcelom) automated cell counter. Next, cells were pelleted by
567 centrifugation (5 min. at 250 × g and RT) and resuspended in isolation buffer (PBS
568 supplemented with 2% heat-inactivated FBS and 1 mM EDTA) at 50 million live cells/ml
569 and filtered through a 35 µm sterile filter cap (Corning #352235) to break apart any
570 aggregated cells. B cells were isolated using StemCell's EasySep Human B Cell
571 Isolation Kit (#17954) according to manufacturer's instruction. After washing with PBS,
572 the isolated B cells were incubated with 1 µl LIVE/DEAD Fixable Aqua Dead Cell Stain
573 Kit (Thermo #L34965) per 1 ml cell suspension, per manufacturer's instructions. After
574 washing the B cells with cold PBS and resuspending them in 50 µl cold PBS with 1%
575 bovine serum albumin (BSA) (Sigma #A7979), the cells were first stained with 40 nM of
576 decoy tetramer (10 min. in the dark on ice) and then with 20 nM of MSP1 tetramer (30
577 min. in the dark on ice), followed by a wash with 1 ml of cold PBS/1% BSA (5 min. at

250 × g and RT). Tetramer-bound B cells were selected using StemCell's EasySep Human PE Positive Selection Kit (#17664) and subsequently stained on ice for 30 min. with an antibody panel against B cell surface markers (**Supplementary table 4**). UltraComp eBeads (Thermo #01222242) were used to prepare compensation controls for each fluorophore per manufacturer's instructions. Before acquisition on a BD FACSAria II cell sorter, the cells were washed with 3 ml of cold PBS with 1% BSA (5 min. at 250 × g and 4°C), diluted to 20 – 30 million cells/ml in PBS with 1% BSA, and filtered into a FACS tube with filter cap. Lymphocytes were gated using forward and sideward scatter, followed by doublet exclusion and gating on live cells. MSP1-specific mature $IgG^+$ and $IgM^+$ B cells ($CD19^+$, $CD20^+$) were gated ($PE^+$, $AF647^-$) and single cells were sorted into 100 µl IMDM/Glutamax/10% FBS in a well of a 96-well plate (Corning #353072). One day prior to the sort, each well was seeded with 30,000 adherent, CD40L-expressing 3T3 cells (kind gift from Dr. Mark Connors, NIH) in 100 µl IMDM/Glutamax/10% FBS containing 2× MycoZap Plus-PR (Lonza #VZA-2021), 100 ng/ml human IL-2 (GoldBio #1110-02-50), 100 ng/ml human IL-21 (GoldBio #1110-21-10), 5 µg/ml TLR9-activator ODN2006 (IDT DNA, sequence TCGTCGTTTTGTCGTTTTGTCGTT), and 60 µg/ml transferrin (Sigma #616424) to promote expansion and differentiation of B cells into antibody-secreting cells (54, 55). After incubation at 37°C and 8% $CO_2$ for two weeks, the wells were screened for the production of IgM or IgG by enzyme-linked immunosorbent assay (ELISA).

**Enzyme-linked immunosorbent assays**

To detect IgG and IgM, 96-well ELISA plates (Corning #3361) were coated with either goat anti-human IgG (Sigma #I2136) or IgM (Sigma #I1636) antibody at a concentration of 4 and 8 µg/ml, respectively, diluted in PBS, at a total volume of 100 µl per well. After a one hour incubation at 37°C or O/N at 4°C, each well was washed once using slowly running (approximately 900 ml / min.) deionized water. This washing method resulted in significantly higher specificity than other methods tested in the lab (using a plate washer with water or PBS containing 0.1% tween-20, or a squeeze bottle filled with PBS containing 0.1% tween-20). All subsequent washes were performed this way. 150 µl blocking buffer (one-third Non-Animal Protein (NAP)-Blocker (G-Biosciences #786-190P) and two-thirds PBS) was added to each well to prevent non-specific binding. After one hour of incubation at 37°C, the wells were washed three times and 50 µl B cell culture supernatant diluted 1:1 in dilution buffer (1% NAP Blocker in PBS; total volume 100 µl) was added per well. Plates were incubated for two hours at 37°C and washed five times. Then, either 100 µl 1:2500 diluted (1% NAP Blocker in PBS) HRP-conjugated anti-human IgG antibody (BioLegend #410902) or 1:5000 HRP-conjugated anti-human IgM antibody (Sigma #AP114P) was added to each well. After incubation for one hour at 37°C and three washes, HRP activity was detected using 50 µl TMB (Thermo #PI34024). Plates were incubated in the dark at RT and the oxidation reaction was stopped by adding 50 µl 0.18M $H_2SO_4$ (Fisher #FLA300-212) per well when the negative controls (wells that received buffer when test wells received culture supernatant) started to color. Absorbance was measured at 450 nm using a BioTek Synergy H4 microplate reader. A human IgG (Sigma #I2511) or IgM (Sigma #I8260-1MG) standard curve (ten three-fold serial dilutions starting at 20 µg/ml) was used to

quantify samples. Wells with values >27 ng/ml were considered positive. This cutoff was determined based on our observation that the amplification of heavy and light chain variable regions always failed from cultures with a lower concentration.

ELISAs to confirm reactivity of MSP1-specific antibodies were performed as described above with the following modifications. Plates were coated with 50 µl in-house produced $MSP1_{3D7}$ per well at a concentration of 16 µg/ml (0.8 µg/well). Coated plates were incubated for 1 hour at 37ºC or overnight at 4°C and all subsequent incubations were done at RT instead of 37°C. To prevent non-specific binding, the wells were blocked with 200 µl PBS containing 0.1% tween-20 and 3% non-fat milk powder (SACO), which significantly increased specificity of the assay (compared to NAP blocker). After discarding the blocking buffer from the wells, the plates were not washed. Purified antibodies were tested at a final concentration of 2.5 µg/ml in 100 – 200 µl in PBS containing 0.1% tween-20 and 1% non-fat milk powder. The plates were washed six times prior to adding the detection antibody, and four times prior to adding TMB substrate. To analyze binding affinity of monoclonal antibodies to $MSP1_{3D7}$, chaotropic ELISAs were performed similar to the above descriptions, with the following modifications. Wells were coated with 0.2 µg protein and the final concentration of the antibodies that were tested was 0.5 µg/ml. Following the incubation with anti-MSP1 antibodies, the plates were washed four times. Then, urea (Fisher #U15-500) was added to wells at the following concentrations: 0, 1, 2, 3, 4, 5 and 8M (in 100 µl PBS with 0.1% tween-20 and 1% milk powder). After a 15-minute incubation at RT, plates were washed four times. The $IC_{50}$ (the molar concentration of urea required to reduce

antibody binding to MSP1 by 50%) was calculated using non-linear regression analysis in GraphPad Prism 9. Urea concentrations were log-transformed prior to analysis. OD values for each technical replicate were normalized by setting the smallest OD to 0% and the largest OD to 100%. The $IC_{50}$ values of three technical replicates were averaged to obtain the final $IC_{50}$ for an experiment.

ELISAs to detect antibody reactivity against merozoites were performed as described for MSP1-specific antibodies above with the following modifications. Free merozoites were coated at 500,000 merozoites per well in 100 µl PBS, followed by overnight incubation at 4°C. Merozoite count was estimated based on culture parasitemia. Plasma samples were tested at a 1:200 dilution in a total volume of 100 µl.

**Amplification of antibody heavy and light chain variable regions**

MSP1-specific B cells that successfully expanded in culture were collected by centrifugation (5 min. at 250 × g and RT) and stored at -70°C in 50 µl Tri-Reagent (Zymo #R2050-1-200). Heavy and light chain variable regions were amplified from MSP1-specific B cells by cDNA synthesis and a series of PCR reactions, shown in **Supplementary figure 4A**. All primer sequences can be found in **Supplementary table 5**. mRNA was isolated using Zymo's Direct-zol RNA Microprep kit (#R2060), eluted in 15 µl elution buffer and then mixed with 0.7 µl reverse primer (10 µM, 200 mM final concentration (f/c) in 35 µl PCR reaction volume) specific for the IgG, or IgM, heavy chain (primers #7 and #297) plus 0.7 µl light chain specific reverse primers (10 µM):

#108 and #109,), and incubated for two minutes at 65°C. Single stranded cDNA was synthesized immediately by adding 0.7 µl SMARTScribe reverse transcriptase (100 U/µl, f/c 2 U/µl, Takara Bio #639537), 7 µl First-Strand buffer (f/c 1×), 7 µl DTT (20 mM, f/c 4 mM), 0.7 µl dNTPs (10 mM each, f/c 200 µM each, Sigma #DNTP-10), 1.75 µl RNase OUT (40 U/µl, f/c 2 U/µl, Thermo #10777019), 0.7 µl template switch oligo (TSO) (10 µM, f/c 200 nM, IDT DNA; #110, **Supplementary table 5**), nuclease-free water till 35 µl and subsequent incubation at 42°C for 2 hours. The TSO was designed with two isodeoxynucleotides at the 5' end to prevent TSO concatemerization and three riboguanosines at the 3' end for increased binding affinity to the appended deoxycytidines (property of the Takara reverse transcriptase) (56, 57). The single-stranded cDNA was immediately purified using Zymo's RNA Clean & Concentrator kit (#R1016) using Zymo's appended protocol to purify fragments >200 nucleotides and was eluted in 10 µl elution buffer. This critical clean-up step ensured that any unused TSO was removed, preventing it from inhibiting the subsequent PCR reactions by serving as template for the forward primer. Immediately after, heavy and light chain variable regions were amplified by PCR in one reaction mix using 8.5 µl purified cDNA, 10 µl AccuStart II PCR SuperMix (QuantaBio #95137), 0.9 µl 10 µM forward primer #106 (f/c 0.45 µM, **Supplementary table 5**), and 0.2 µl of the reverse primers (10 µM) used to synthesize the cDNA (#7, #297, #108, and #109, each at f/c 0.1 µM). Cycling conditions were 94°C for 3 min., 35 cycles of 30 sec. at 94°C, 30 sec. at 55°C and 35 sec. at 72°C, followed by 5 min. at 72°C. A second, nested amplification was required to obtain enough amplicon DNA, and was done separately for heavy chain, kappa light chain, and lambda light chain variable regions, using AccuStart II PCR SuperMix, and 2

691 µl of the first, unpurified PCR as template in a total reaction volume of 20 µl. Mixes of
692 primers (**Supplementary figure 4A**) as described by Hua-Xin Liao *et al*. (58) were used
693 for this second PCR, with a final concentration of 0.1 µM for each individual primer.
694 Reverse primer #67 was added for the heavy chain variable region PCR to allow for
695 amplification of variable regions originating from $IgG_2$, $IgG_3$ and $IgG_4$ mRNA, in addition
696 to #30 which was specific for $IgG_1$. Cycling conditions were as described above, except
697 for the extension step (shortened to 30 sec.) and the annealing step, which was 30 sec.
698 at 60°C for the IgG1 heavy chain variable region, 30 sec. at 63ºC for the IgM heavy
699 chain variable region, and 30 sec. at 50°C for the light chain variable regions.

700

701 Linear IgG expression cassettes (58) were synthesized by PCR using 3 overlapping
702 DNA fragments: a promoter (705 bp), a variable region and a constant region ($IgG_1$
703 heavy chain: 1188 bp; pentameric $IgG_1$ heavy chain: 1326 bp; kappa light chain: 568
704 bp; lambda light chain: 534 bp). Details about the assembly of linear expression
705 cassettes are described by Liao *et*. *al*. (58). All fragments were amplified in a 100 µl
706 reaction using 20 ng plasmid template (HV0023 – HV0026 (58) or the $IgG_1$ expression
707 plasmid containing the IgM multimerization sequence (see below)), 4 µl forward primer
708 (10 µM), 4 µl reverse primer (10 µM), and QuantaBio AccuStart II PCR supermix (2×)
709 using the following cycling program: 94ºC for 3 min., 35 cycles of (94ºC for 30 sec.,
710 68ºC for 30 sec., and 72ºC for 40 – 75 sec. (1 min. per 1000 bp)) and 72ºC for 5 min.
711 Primers 53 and 54 were used for the promoter fragment, 55 and 58 for the heavy chain
712 constant region fragment, 56 and 58 for the kappa light chain constant region fragment,
713 57 and 58 for the lambda light chain constant region fragment, and 55 and 494 for the

pentameric $IgG_1$ heavy chain constant region fragment (**Supplementary table 5**). The overlapping PCRs were done as follows. The cycling program was the same for all overlapping PCRs: 98ºC for 1 min., 30× (98ºC for 20 sec., 68ºC for 15 sec., 72ºC for 60 sec.), 72ºC for 10 min. Two ng of each fragment (promoter, constant region, variable region) was used as template in a 25 µl PCR reaction with 2× KAPA HiFi Hot Start Ready Mix (Roche #KK2602) and 1 µl (10 µM) of the following forward and reverse primers: 50 and 51 for the IgG1 heavy chain, 50 and 52 for the kappa and lambda light chain, and 50 and 469 for the $IgG_1$ heavy chain with IgM multimerization domain (**Supplementary table 5**). The final size of the linear expression cassettes was ~2300 bp for the IgG1 heavy chain, ~2400 bp for the IgG1 heavy chain with IgM multimerization domain, and 1600 bp for the kappa and lambda light chains (**Supplementary figure 4B**). All linear expression cassettes were purified and sequence verified by Sanger sequencing. Variable region sequences were analyzed with IMGT/V-QUEST (28) using default settings to identify V(D)J gene usage and amino acid substitutions.

**Generation of antibody expression plasmids**

Antibody variable regions were cloned into expression plasmids from Invivogen (#pfusess-hchg1, #pfuse2ss-hclk, #pfuse2ss-hcll2). The variable heavy and light chain regions were amplified from the linear expression cassettes (2 µl at 1 ng/µl) using 10 µl NEB Q5 Hot Start HiFi PCR master mix (#M0494S), 6 µl nuclease-free water and 1 µl sequence-specific F and R primer (10 µM, f/c 500 nM) that were based on the results of analysis using IMGT/VQUEST (28). These primers introduced restriction sites (EcoRI &

737 NheI for hchg1, EcoRI & BsiWII for hclk, and EcoRI & AvrII for hcll2). Annealing
738 temperatures were primer sequence dependent and were calculated using NEB's Tm
739 calculator to match the salt concentration in their buffer. In an attempt to express the
740 variable regions from $IgM^+$ B cells as a multimer (pentamer/hexamer mix) instead of a
741 monomer, we modified the $IgG_1$ heavy chain expression plasmid (15). The IgM
742 multimerization sequence PTLYNVSLVMSDTAGTCY
743 (CCAACGCTCTATAATGTCTCTTTGGTTATGTCCGACACAGCCGGTACCTGCTAT)
744 was cloned into the $IgG_1$ expression vector at the C-terminus of the open reading frame,
745 immediately in front of the stop codon, and the leucine at position -139 relative to the
746 proline in the multimerization sequence was changed into a cysteine. Every plasmid
747 was Sanger sequence-verified prior to using it as expression vector.

748

749 **Antibody expression and purification**

750 For small scale screening, one ml Expi293F cell cultures in a 6 well plate were
751 transfected with heavy and light chain linear expression cassettes (1:1 molar ratio)
752 according to the manufacturer's instructions for 25 – 30 ml cultures (also at 125 rpm).
753 Heavy and light chain antibody expression plasmids were used at a molar ratio of 1:2 to
754 transfect 5 ml cultures. The antibodies were purified from the culture supernatant 4 – 6
755 days later using protein G magnetic beads (Promega #G7472). Purified antibodies and
756 antibody elution buffer (5 parts elution buffer (100 µM glycine-HCl, pH 2.7) and 1 part
757 neutralization buffer (2M Tris buffer, pH 7.5)) were buffer exchanged to PBS using 100
758 kDa cutoff Protein Concentrators (Thermo #88523). The samples were diluted > 50,000
759 × in PBS by repeated centrifugation at 4,000 × g and 4ºC. Purified antibodies were

quantified using the Coomassie Plus (Bradford) Assay Kit (Thermo #23236) on a NanoDrop One spectrophotometer, according to the manufacturer's instructions, and visualized on SDS-PAGE gel with a standard amount of BSA to confirm protein size and purity (**Supplementary figure 3B**).

**Parasite culture and merozoite isolation**

*P. falciparum* 3D7 strain parasites were cultured (59) in human $AB^+$ erythrocytes (Interstate Blood Bank, Memphis, TN, USA) at 3 – 10% parasitemia in complete culture medium (5% hematocrit). Complete culture medium consisted of RPMI 1640 medium (Gibco #32404014) supplemented with gentamicin (45 µg/ml final concentration; Gibco #15710064), HEPES (40 mM; Fisher #BP3101), $NaHCO_3$ (1.9 mg/ml; Sigma #SX03201), NaOH (2.7 mM; Fisher #SS266-1), hypoxanthine (17 µg/ml; Alfa Aesar #A11481-06), L-glutamine (2.1 mM; Corning #25005CI), D-glucose (2.1 mg/ml; Fisher #D16-1), and 10% heat-inactivated human $AB^+$ serum (Valley Biomedical #HP1022). Parasites were cultured at 37°C in an atmosphere of 5% $O_2$, 5% $CO_2$, and 90% $N_2$. Before use in cultures, 12.5 ml packed erythrocytes were washed twice with 10 ml cold incomplete medium (complete culture medium without human serum) and pelleted between each wash by centrifugation at 500 × g for 8 min. at 4°C (max. acceleration and weakest break). Washed erythrocytes were resuspended in 2 volumes of complete medium and stored at 4°C.

781 Parasites were synchronized to the ring stage by treatment with 5% D-sorbitol (60)
782 (Fisher #S459-500). Cultures containing high percentages of ring-stage parasites were
783 centrifuged at 250 × g for 5 min. at RT. Pelleted erythrocytes were resuspended in 10
784 volumes of 5% D-sorbitol in MQ water, vortexed for 30 sec. and incubated for 8 min. at
785 37°C. The cells were then washed with 5 volumes of complete culture medium (250 × *g*
786 for 5 min. at RT) and resuspended in complete culture medium at 5% hematocrit and
787 cultured as described above. To obtain tightly synchronized parasites, sorbitol
788 treatments were performed twice, 14 hours apart.
789 Infected erythrocytes containing parasites in the late-trophozoite and schizont stages
790 were isolated from culture by magnetic separation (61, 62). Late-stage parasites were
791 separated from uninfected and ring-infected erythrocytes with a SuperMACS II
792 Separator (Miltenyi #130-044-104). The magnet was assembled with a D column
793 (Miltenyi #130-041-201) according to manufacturer's instructions. The column was
794 equilibrated with 200 ml incomplete medium. An additional 50 ml incomplete medium
795 was added to the column through the side syringe to remove air bubbles possibly
796 remaining in the column matrix. A 22 G needle (BD #305155) was attached to the
797 stopcock to serve as a flow restrictor. For safety purposes the plastic protective sheath
798 remained on the needle after cutting the end to allow flow of the liquid without exposing
799 the tip of the needle. Approximately 100 – 200 ml of synchronized parasite culture (5 –
800 10% parasitemia, 5% hematocrit) 24 – 27 hours following the second sorbitol treatment
801 (majority of parasites in the early segmented schizont stage, 4 – 6 nuclei visible by
802 Giemsa staining) were used for merozoite isolation. After passing the parasite culture
803 through the column, the column was washed from the top with incomplete medium until

804 the flowthrough was clear (usuall ~100 ml). Next, the column was washed with a total of
805 150 ml incomplete medium (50 ml from the side and 100 ml from the top). Erythrocytes
806 containing late-stage parasites with high paramagnetic hemozoin levels are
807 preferentially retained in the column matrix while attached to the magnet (63) allowing
808 for separation of late-stage parasites from uninfected erythrocytes and early-stage
809 parasites. The column was removed from the magnet and 60 ml incomplete medium
810 was used to elute the erythrocytes from the column matrix. The erythrocytes were
811 pelleted by centrifugation at 250 × *g* for 5 min. at RT and were resuspended in 3 ml
812 complete culture medium. Infected erythrocytes were incubated with E64 (10 µM final
813 concentration, Sigma #324890-1MG) for 8 hours at normal culture conditions to allow
814 the parasites to develop into fully segmented schizonts while preventing egress from the
815 erythrocytes. Infected erythrocytes containing schizonts were then pelleted by
816 centrifugation at 1,900 × *g* for 8 min. at RT and the supernatant containing E64 was
817 removed. A thin smear from the pellet was Giemsa stained and merozoite yield was
818 assessed by counting the number of fully segmented schizonts present. The pellet was
819 resuspended in 4 ml incomplete medium. Merozoites were released from the
820 erythrocytes by passing them through a 1.2 µm syringe filter (Pall #4190) and were
821 subsequently pelleted by centrifugation at 4,000 × *g* for 10 min. at RT. On average, 5 ×
822 $10^7$ merozoites were collected per 25 ml of synchronized culture. The merozoites were
823 resuspended in PBS and stored at 4°C for up to one day until used for the ELISA.

824

825 **Immunofluorescence assay**

826 All steps of the immunofluorescence assay were done at RT. A thin blood smear was
827 made on a microscopy slide from a 1 µl drop of E64-treated schizont culture. After
828 drying for 30 sec., the cells were fixed by loading 1 ml of 4% paraformaldehyde
829 (Electron Microscopy #15710) on the slide and incubating it for 30 min. The fixed cells
830 were then washed three times with 1 ml PBS. Following the washes, the cells were
831 permeabilized with 0.1% Triton-X (Fisher # BP151) in PBS and incubated for 30 min.
832 The cells were then washed for an additional three washes using PBS. The slide was
833 treated with blocking buffer (2% BSA, 0.05% Tween-20, 100 mM Glycine, 3 mM EDTA
834 and 150 mM NaCl in PBS) for one hour. MSP1-specific mAbs were added to the cells at
835 1 µg/ml in 500 µl blocking buffer and incubated for one hour. Samples were then
836 washed again three times using PBS. Goat anti-human IgG conjugated to FITC
837 (Thermo #A18830) secondary antibody was diluted 1:1000 (1.5 µg/ml) in blocking buffer
838 and then added to the smear to incubate for one hour in the dark. Samples were again
839 washed three times using PBS in the dark and then allowed to air dry for one hour in the
840 dark. Slides were mounted using 10 µl ProLong Glass mounting medium containing
841 NucBlue Stain (Thermo #P36985) and sealed with a cover slip. Samples were imaged
842 using a Zeiss Axio Imager Z1 with Zen Blue software.

843

844 **Luminex assay**

845 100 pmol $MSP1_{3D7}$, $MSP1_{Dd2}$, $MSP1_{HB3}$, and SARS-CoV-2 receptor binding domain
846 were coupled per 1 × $10^6$ MagPlex microspheres (Luminex, #MC10025-ID) using the
847 Luminex protein coupling kit (#40-50016) per manufacturer's instructions. All
848 subsequent steps were done at RT and the beads were protected from light using

aluminum foil. Coupled beads were pooled, resuspended in buffer A (PBS with 0.05% Tween 20 (Fisher #BP337), 0.5% BSA (Sigma #A7979), 0.02% sodium azide) and plated at 1000 beads per well for each protein in a black, flat-bottom 96 well plate (Bio-Rad #171025001). The beads were washed once. All washes were done with 100 µl PBST (PBS with 0.05% Tween 20) using a handheld magnetic washer (Bio-Rad #171020100). The incubation time on the magnet was always 2 min. Next, the beads were incubated with 50 µl purified anti-MSP1 antibody (diluted to 1 µg/ml using buffer B) or B cell culture supernatant (diluted 1:1 with buffer B) for 30 min. with constant agitation (500 rpm, 2.5 mm orbital diameter). Buffer B (0.05% Tween-20, 0.5% BSA, 0.02% sodium azide, 0.1% casein (Sigma #C7078), 0.5% PVA (Sigma #P8136) and 0.5% PVP (Sigma #PVP360), 15 µg/ml *E. coli* lysate) was prepared a day prior to the assay since it required the chemicals to dissolve O/N. On the day of the assay, *E. coli* lysate (MCLAB #ECCL-100) was resuspended in MQ water and added to a final concentration of 15 µg/ml. Prior to use, buffer B was centrifuged at 10,000 × g for 10 min. After three washes, 50 µl secondary antibody diluted in buffer A (PE anti-human IgG (1:200 dilution; Jackson ImmunoResearch #109-116-098)) or PE anti-human IgM (1:80 dilution; BioLegend #314507)) was added per well. After 30 min. incubation with constant agitation, the beads were washed three times and subsequently incubated in 50 µl buffer A for 30 min. with constant agitation. After one final wash, the beads were resuspended in 100 µl PBS and fluorescence intensity was measured using a calibrated and validated Bio-Rad Bio-Plex 200 machine.

**Growth inhibition assay**

*P. falciparum* isolate 3D7 parasites were pre-synchronized at the ring stage with a 5% D-sorbitol (Fisher #S459-500) treatment as described above, followed four days later by two additional 5% D-sorbitol treatments 14 hours apart (60). At the late trophozoite / early schizont stage (24 hours after the third D-sorbitol treatment), parasitemia was determined by inspection of a Giemsa-stained blood smear. The smear was also used to confirm correct parasite staging. Immediately after, 20 µl of each antibody (1 mg/ml in PBS) was added to wells containing 30 µl complete medium in a black clear bottom 96-well plate (Corning #3603). A monoclonal antibody specific for apical membrane antigen 1 (AMA1) was used as a positive control (BEI #MRA-481A). Antibody elution buffer (100 mM glycine-HCl, pH 2.7) that was buffer exchanged to PBS alongside purified antibodies (see "Antibody expression and purification" above) was used as a negative control. Fifty µl parasite culture (1% parasitemia and 2% hematocrit) was then added to wells containing antibody or negative control. Uninfected erythrocytes (2% hematocrit) were used to determine the background signal. The plate was then incubated at standard parasite culture conditions (described above) for 48 hours before being transferred to a -70°C freezer. After overnight incubation of the plate at -70°C, SYBR green dye (Invitrogen #S7585) was added to lysis buffer (20 mM Tris-HCl (pH7.5), 5 mM EDTA, 0.008% saponin (Sigma # 558255100GM), 0.08% Triton X-100 in MQ water) at 0.2 µl dye per ml of lysis buffer. One hundred µl SYBR green lysis buffer was added to each well and the plate was incubated in the dark at 37°C for 3 – 6 hours. Fluorescence (excitation = 495 nm, emission = 525 nm, cutoff = 515 nm) was measured with a BioTek Synergy H4 plate reader. The instrument was programmed to read the plate from the bottom after mixing for 5 sec. The average background fluorescence

value was subtracted from the fluorescence signal of the wells with infected cells. Percent growth inhibition was expressed as the reduction in fluorescence signal in wells incubated with antibody as compared to the negative control.

**Plasma antibody proteomics**

Total IgG was isolated from 1 ml plasma using Protein G Plus Agarose (Thermo #22851) affinity chromatography and cleaved into $F(ab')_2$ fragments using IdeS protease. MSP1-specific $F(ab')_2$ was isolated by affinity chromatography using 1 mg recombinant $MSP1_{19}$ produced in *E. coli* (Meridian Life Sciences, #R01603 and #R01604) coupled to 0.05 mg dry NHS-activated agarose resin (Thermo #26196) as follows. $F(ab')_2$ (10 mg/ml in PBS) was rotated at 8 rpm with antigen-conjugated affinity resin for 1 hour at RT, loaded into 0.5 ml spin columns (Thermo #89868), washed 12× with 0.4 ml Dulbecco's PBS (1,000 × *g* for 30 sec. at RT), and eluted with 0.5 ml fractions of 1% formic acid. IgG-containing elution fractions were concentrated to dryness in a speed-vac, resuspended in $ddH_2O$, combined, neutralized with 1M Tris / 3M NaOH, and prepared for liquid chromatography–tandem mass spectrometry (LC-MS/MS) as described previously (64, 65) with the modifications that (i) peptide separation using acetonitrile gradient was run for 120 min and (ii) data was collected on an Orbitrap Fusion (Thermo Fisher Scientific) operated at 120,000 resolution using HCD (higher-energy collisional dissociation) in topspeed mode with a 3 sec. cycle time. B cell receptor sequencing data was available from a previous study (30). Demultiplexing of sequence reads and the generation of consensus sequences for UMI groups were performed as outlined by Turchaninova *et al.* using software tools MIGEC (v1.2.9) and

MiTools (v1.5) (66). Sequences with ≥2 reads were clustered into clonal lineages defined by 90% HCDR3 amino acid identity using USEARCH (67). LC-MS/MS search databases were prepared as previously described (64), using custom Python scripts (available upon request). MS searches, and MS data analyses were performed as previously described (64, 65), adjusting the stringency of the elution XIC:flowthrough XIC filter to 2:1.

## Data visualization and statistics

Flow cytometry data were analyzed and plotted using FlowJo (v10.7.1). Dot plots were generated using the package ggplot2 in RStudio (v1.4.1103) using R (v4.0.4). All other plots were generated in GraphPad Prism 9, which was also used for statistical analyses. The statistical test used for each analysis is indicated in the figure legends.

## Data availability statement

The BCR-seq data set analyzed in the current study is available in the NCBI SRA repository under accession numbers SAMN17497575-7.

## Conflict of interest

The authors declare that the research was conducted in the absence of any commercial or financial relationships that could be construed as a potential conflict of interest.

## Author contributions

EMB secured funding for the study, conceived the research question, and designed the study. SJG performed flow cytometry. SJG, KC, and SB produced recombinant antigens and monoclonal antibodies and contributed to other experiments. GB performed IFA and growth-inhibition assays. RAR, RG, and AEB performed merozoite ELISAs. AEB generated BCR-seq data. KCG and GCI performed plasma IgG proteomics. IS and BG provided clinical samples and data. SJG, SB, and EMB wrote the manuscript with input from all other co-authors.

## Funding

This work was supported by National Institutes of Health/National Institute of Allergy and Infectious Diseases (R01 AI153425 to E.M.B.). S.J.G and A.E.B. were supported by Graduate Research in Immunology Program training grant NIH T32 AI138944. R.A.R. was supported by Translational Science Training award TL1 TR002647. Data were generated in the Flow Cytometry Shared Resource Facility, which is supported by UT Health, NIH-NCI P30 CA054174-20 (CTRC at UT Health) and UL1 TR001120 (CTSA grant) and in the Genome Sequencing Facility, which is supported by UT Health San Antonio, NIH-NCI P30 CA054174 (Cancer Center at UT Health San Antonio), NIH Shared Instrument grant 1S10OD021805-01 (S10 grant), and CPRIT Core Facility Award (RP160732).

## Abbreviations

| | |
|---|---|
| BCR | B cell receptor |
| HCDR3 | heavy chain complementarity determining region 3 |
| Ig | immunoglobulin |
| MBC | memory B cell |
| mAb | monoclonal antibody |

## Acknowledgements

We would like to thank Dr. Kevin O. Saunders (Duke Human Vaccine Institute) for sharing reagents and protocols for the expression of recombinant IgG using linear Ig heavy and light chain gene expression cassettes from Liao *et al*. The 3T3-msCD40L cell line was a kind gift from Dr. Mark Connors (National Institute of Allergy and Infectious Diseases). Plasmids encoding 3D7 MSP1-bio, BirA, and rat CD200 were a kind gift from Dr. Gavin Wright, (Wellcome Sanger Institute; Addgene plasmids # 47709, 32408, and 36152). The following reagents were obtained through BEI Resources, NIAID, NIH: *Plasmodium falciparum*, Strain 3D7, MRA-102, contributed by Dr. Daniel J. Carucci; and Monoclonal Antibody N4-1F6 Anti-*Plasmodium falciparum* Apical Membrane Antigen 1 (AMA1) (produced *in vitro*), MRA-481A, contributed by Dr. Carole A. Long.

## References

1. World Health Organization. World malaria report 2020. *World Health Organization, Geneva, Switzerland.* 2020.

2. Rts SCTP. Efficacy and safety of RTS,S/AS01 malaria vaccine with or without a booster dose in infants and children in Africa: final results of a phase 3, individually randomised, controlled trial. *Lancet.* 2015;386(9988):31-45.

985 3. Neafsey DE, Juraska M, Bedford T, Benkeser D, Valim C, Griggs A, et al. Genetic
986 Diversity and Protective Efficacy of the RTS,S/AS01 Malaria Vaccine. *N Engl J*
987 *Med.* 2015;373(21):2025-37.

988 4. Yman V, White MT, Asghar M, Sundling C, Sonden K, Draper SJ, et al. Antibody
989 responses to merozoite antigens after natural Plasmodium falciparum infection:
990 kinetics and longevity in absence of re-exposure. *BMC Med.* 2019;17(1):22.

991 5. Hill DL, Wilson DW, Sampaio NG, Eriksson EM, Ryg-Cornejo V, Harrison GLA, et
992 al. Merozoite Antigens of Plasmodium falciparum Elicit Strain-Transcending
993 Opsonizing Immunity. *Infect Immun.* 2016;84(8):2175-84.

994 6. Fowkes FJ, Richards JS, Simpson JA, and Beeson JG. The relationship between
995 anti-merozoite antibodies and incidence of Plasmodium falciparum malaria: A
996 systematic review and meta-analysis. *PLoS Med.* 2010;7(1):e1000218.

997 7. Boyle MJ, Reiling L, Feng G, Langer C, Osier FH, Aspeling-Jones H, et al. Human
998 antibodies fix complement to inhibit Plasmodium falciparum invasion of erythrocytes
999 and are associated with protection against malaria. *Immunity.* 2015;42(3):580-90.

1000 8. Osier FH, Fegan G, Polley SD, Murungi L, Verra F, Tetteh KK, et al. Breadth and
1001 magnitude of antibody responses to multiple Plasmodium falciparum merozoite
1002 antigens are associated with protection from clinical malaria. *Infect Immun.*
1003 2008;76(5):2240-8.

1004 9. Osier FH, Feng G, Boyle MJ, Langer C, Zhou J, Richards JS, et al. Opsonic
1005 phagocytosis of Plasmodium falciparum merozoites: mechanism in human
1006 immunity and a correlate of protection against malaria. *BMC Med.* 2014;12:108.

1007 10. Stanisic DI, Fowkes FJ, Koinari M, Javati S, Lin E, Kiniboro B, et al. Acquisition of
1008 antibodies against Plasmodium falciparum merozoites and malaria immunity in
1009 young children and the influence of age, force of infection, and magnitude of
1010 response. *Infect Immun.* 2015;83(2):646-60.

1011 11. Richards JS, Arumugam TU, Reiling L, Healer J, Hodder AN, Fowkes FJ, et al.
1012 Identification and prioritization of merozoite antigens as targets of protective human
1013 immunity to Plasmodium falciparum malaria for vaccine and biomarker
1014 development. *J Immunol.* 2013;191(2):795-809.

1015 12. Kana IH, Singh SK, Garcia-Senosiain A, Dodoo D, Singh S, Adu B, et al. Breadth of
1016 Functional Antibodies Is Associated With Plasmodium falciparum Merozoite
1017 Phagocytosis and Protection Against Febrile Malaria. *J Infect Dis.* 2019;220(2):275-
1018 84.

1019 13. Reiling L, Boyle MJ, White MT, Wilson DW, Feng G, Weaver R, et al. Targets of
1020 complement-fixing antibodies in protective immunity against malaria in children. *Nat*
1021 *Commun.* 2019;10(1):610.

14. Boyle MJ, Chan JA, Handayuni I, Reiling L, Feng G, Hilton A, et al. IgM in human immunity to Plasmodium falciparum malaria. *Sci Adv.* 2019;5(9):eaax4489.

15. Thouvenel CD, Fontana MF, Netland J, Krishnamurty AT, Takehara KK, Chen Y, et al. Multimeric antibodies from antigen-specific human IgM+ memory B cells restrict Plasmodium parasites. *J Exp Med.* 2021;218(4).

16. Hopp CS, Sekar P, Diouf A, Miura K, Boswell K, Skinner J, et al. Plasmodium falciparum-specific IgM B cells dominate in children, expand with malaria, and produce functional IgM. *J Exp Med.* 2021;218(4).

17. Akkaya M, Kwak K, and Pierce SK. B cell memory: building two walls of protection against pathogens. *Nat Rev Immunol.* 2020;20(4):229-38.

18. Crompton PD, Kayala MA, Traore B, Kayentao K, Ongoiba A, Weiss GE, et al. A prospective analysis of the Ab response to Plasmodium falciparum before and after a malaria season by protein microarray. *Proc Natl Acad Sci U S A.* 2010;107(15):6958-63.

19. Weiss GE, Traore B, Kayentao K, Ongoiba A, Doumbo S, Doumtabe D, et al. The Plasmodium falciparum-specific human memory B cell compartment expands gradually with repeated malaria infections. *PLoS Pathog.* 2010;6(5):e1000912.

20. Holder AA. The carboxy-terminus of merozoite surface protein 1: structure, specific antibodies and immunity to malaria. *Parasitology.* 2009;136(12):1445-56.

21. Ghoshal S, Gajendra P, Datta Kanjilal S, Mitra M, and Sengupta S. Diversity analysis of MSP1 identifies conserved epitope organization in block 2 amidst high sequence variability in Indian Plasmodium falciparum isolates. *Malar J.* 2018;17(1):447.

22. Dent AE, Nakajima R, Liang L, Baum E, Moormann AM, Sumba PO, et al. Plasmodium falciparum Protein Microarray Antibody Profiles Correlate With Protection From Symptomatic Malaria in Kenya. *J Infect Dis.* 2015;212(9):1429-38.

23. Ogutu BR, Apollo OJ, McKinney D, Okoth W, Siangla J, Dubovsky F, et al. Blood stage malaria vaccine eliciting high antigen-specific antibody concentrations confers no protection to young children in Western Kenya. *PLoS One.* 2009;4(3):e4708.

24. Sheehy SH, Duncan CJ, Elias SC, Choudhary P, Biswas S, Halstead FD, et al. ChAd63-MVA-vectored blood-stage malaria vaccines targeting MSP1 and AMA1: assessment of efficacy against mosquito bite challenge in humans. *Mol Ther.* 2012;20(12):2355-68.

25. Kamya MR, Arinaitwe E, Wanzira H, Katureebe A, Barusya C, Kigozi SP, et al. Malaria transmission, infection, and disease at three sites with varied transmission intensity in Uganda: implications for malaria control. *Am J Trop Med Hyg.* 2015;92(5):903-12.

1059 26. Taylor JJ, Martinez RJ, Titcombe PJ, Barsness LO, Thomas SR, Zhang N, et al.
1060 Deletion and anergy of polyclonal B cells specific for ubiquitous membrane-bound
1061 self-antigen. *J Exp Med.* 2012;209(11):2065-77.

1062 27. Krishnamurty AT, Thouvenel CD, Portugal S, Keitany GJ, Kim KS, Holder A, et al.
1063 Somatically Hypermutated Plasmodium-Specific IgM(+) Memory B Cells Are Rapid,
1064 Plastic, Early Responders upon Malaria Rechallenge. *Immunity.* 2016;45(2):402-14.

1065 28. Alamyar E, Duroux P, Lefranc MP, and Giudicelli V. IMGT((R)) tools for the
1066 nucleotide analysis of immunoglobulin (IG) and T cell receptor (TR) V-(D)-J
1067 repertoires, polymorphisms, and IG mutations: IMGT/V-QUEST and IMGT/HighV-
1068 QUEST for NGS. *Methods Mol Biol.* 2012;882:569-604.

1069 29. Andrews SF, Chambers MJ, Schramm CA, Plyler J, Raab JE, Kanekiyo M, et al.
1070 Activation Dynamics and Immunoglobulin Evolution of Pre-existing and Newly
1071 Generated Human Memory B cell Responses to Influenza Hemagglutinin.
1072 *Immunity.* 2019;51(2):398-410 e5.

1073 30. Braddom AE, Bol S, Gonzales SJ, Reyes RA, Musinguzi K, Nankya F, et al. B Cell
1074 Receptor Repertoire Analysis in Malaria-Naive and Malaria-Experienced Individuals
1075 Reveals Unique Characteristics of Atypical Memory B Cells. *mSphere.*
1076 2021;6(5):e0072621.

1077 31. Miller LH, Roberts T, Shahabuddin M, and McCutchan TF. Analysis of sequence
1078 diversity in the Plasmodium falciparum merozoite surface protein-1 (MSP-1). *Mol*
1079 *Biochem Parasitol.* 1993;59(1):1-14.

1080 32. Tanabe K, Mackay M, Goman M, and Scaife JG. Allelic dimorphism in a surface
1081 antigen gene of the malaria parasite Plasmodium falciparum. *J Mol Biol.*
1082 1987;195(2):273-87.

1083 33. Viant C, Weymar GHJ, Escolano A, Chen S, Hartweger H, Cipolla M, et al.
1084 Antibody Affinity Shapes the Choice between Memory and Germinal Center B Cell
1085 Fates. *Cell.* 2020;183(5):1298-311 e11.

1086 34. Gotz A, Tang MS, Ty MC, Arama C, Ongoiba A, Doumtabe D, et al. Atypical
1087 activation of dendritic cells by Plasmodium falciparum. *Proc Natl Acad Sci U S A.*
1088 2017;114(49):E10568-E77.

1089 35. Pack AD, Schwartzhoff PV, Zacharias ZR, Fernandez-Ruiz D, Heath WR, Gurung
1090 P, et al. Hemozoin-mediated inflammasome activation limits long-lived anti-malarial
1091 immunity. *Cell Rep.* 2021;36(8):109586.

1092 36. Portugal S, Obeng-Adjei N, Moir S, Crompton PD, and Pierce SK. Atypical memory
1093 B cells in human chronic infectious diseases: An interim report. *Cell Immunol.*
1094 2017;321:18-25.

37. Braddom AE, Batugedara G, Bol S, and Bunnik EM. Potential functions of atypical memory B cells in Plasmodium-exposed individuals. *Int J Parasitol.* 2020;50(13):1033-42.

38. Vijay R, Guthmiller JJ, Sturtz AJ, Surette FA, Rogers KJ, Sompallae RR, et al. Infection-induced plasmablasts are a nutrient sink that impairs humoral immunity to malaria. *Nat Immunol.* 2020;21(7):790-801.

39. Kenderes KJ, Levack RC, Papillion AM, Cabrera-Martinez B, Dishaw LM, and Winslow GM. T-Bet(+) IgM Memory Cells Generate Multi-lineage Effector B Cells. *Cell Rep.* 2018;24(4):824-37 e3.

40. Duah NO, Weiss HA, Jepson A, Tetteh KK, Whittle HC, and Conway DJ. Heritability of antibody isotype and subclass responses to Plasmodium falciparum antigens. *PLoS One.* 2009;4(10):e7381.

41. Richards JS, Stanisic DI, Fowkes FJ, Tavul L, Dabod E, Thompson JK, et al. Association between naturally acquired antibodies to erythrocyte-binding antigens of Plasmodium falciparum and protection from malaria and high-density parasitemia. *Clin Infect Dis.* 2010;51(8):e50-60.

42. Acquah FK, Lo AC, Akyea-Mensah K, Abagna HB, Faye B, Theisen M, et al. Stage-specific Plasmodium falciparum immune responses in afebrile adults and children living in the Greater Accra Region of Ghana. *Malar J.* 2020;19(1):64.

43. Walker MR, Knudsen AS, Partey FD, Bassi MR, Frank AM, Castberg FC, et al. Acquisition and decay of IgM and IgG responses to merozoite antigens after Plasmodium falciparum malaria in Ghanaian children. *PLoS One.* 2020;15(12):e0243943.

44. Dodoo D, Aikins A, Kusi KA, Lamptey H, Remarque E, Milligan P, et al. Cohort study of the association of antibody levels to AMA1, MSP119, MSP3 and GLURP with protection from clinical malaria in Ghanaian children. *Malar J.* 2008;7:142.

45. Adu B, Cherif MK, Bosomprah S, Diarra A, Arthur FK, Dickson EK, et al. Antibody levels against GLURP R2, MSP1 block 2 hybrid and AS202.11 and the risk of malaria in children living in hyperendemic (Burkina Faso) and hypo-endemic (Ghana) areas. *Malar J.* 2016;15:123.

46. Ahmed Ismail H, Ribacke U, Reiling L, Normark J, Egwang T, Kironde F, et al. Acquired antibodies to merozoite antigens in children from Uganda with uncomplicated or severe Plasmodium falciparum malaria. *Clin Vaccine Immunol.* 2013;20(8):1170-80.

47. Gonzalez-Quintela A, Alende R, Gude F, Campos J, Rey J, Meijide LM, et al. Serum levels of immunoglobulins (IgG, IgA, IgM) in a general adult population and their relationship with alcohol consumption, smoking and common metabolic abnormalities. *Clin Exp Immunol.* 2008;151(1):42-50.

1133 48. Khan SR, van der Burgh AC, Peeters RP, van Hagen PM, Dalm V, and Chaker L.
1134 Determinants of Serum Immunoglobulin Levels: A Systematic Review and Meta-
1135 Analysis. *Front Immunol.* 2021;12:664526.

1136 49. Cohen S, Mc GI, and Carrington S. Gamma-globulin and acquired immunity to
1137 human malaria. *Nature.* 1961;192:733-7.

1138 50. Roskin KM, Jackson KJL, Lee JY, Hoh RA, Joshi SA, Hwang KK, et al. Aberrant B
1139 cell repertoire selection associated with HIV neutralizing antibody breadth. *Nat*
1140 *Immunol.* 2020;21(2):199-209.

1141 51. Kilama M, Smith DL, Hutchinson R, Kigozi R, Yeka A, Lavoy G, et al. Estimating the
1142 annual entomological inoculation rate for Plasmodium falciparum transmitted by
1143 Anopheles gambiae s.l. using three sampling methods in three sites in Uganda.
1144 *Malar J.* 2014;13:111.

1145 52. Crosnier C, Wanaguru M, McDade B, Osier FH, Marsh K, Rayner JC, et al. A library
1146 of functional recombinant cell-surface and secreted P. falciparum merozoite
1147 proteins. *Mol Cell Proteomics.* 2013;12(12):3976-86.

1148 53. Bushell KM, Sollner C, Schuster-Boeckler B, Bateman A, and Wright GJ. Large-
1149 scale screening for novel low-affinity extracellular protein interactions. *Genome*
1150 *Res.* 2008;18(4):622-30.

1151 54. Huang J, Doria-Rose NA, Longo NS, Laub L, Lin CL, Turk E, et al. Isolation of
1152 human monoclonal antibodies from peripheral blood B cells. *Nat Protoc.*
1153 2013;8(10):1907-15.

1154 55. Lindner JM, Cornacchione V, Sathe A, Be C, Srinivas H, Riquet E, et al. Human
1155 Memory B Cells Harbor Diverse Cross-Neutralizing Antibodies against BK and JC
1156 Polyomaviruses. *Immunity.* 2019;50(3):668-76 e5.

1157 56. Zajac P, Islam S, Hochgerner H, Lonnerberg P, and Linnarsson S. Base
1158 preferences in non-templated nucleotide incorporation by MMLV-derived reverse
1159 transcriptases. *PLoS One.* 2013;8(12):e85270.

1160 57. Kapteyn J, He R, McDowell ET, and Gang DR. Incorporation of non-natural
1161 nucleotides into template-switching oligonucleotides reduces background and
1162 improves cDNA synthesis from very small RNA samples. *BMC Genomics.*
1163 2010;11:413.

1164 58. Liao HX, Levesque MC, Nagel A, Dixon A, Zhang R, Walter E, et al. High-
1165 throughput isolation of immunoglobulin genes from single human B cells and
1166 expression as monoclonal antibodies. *J Virol Methods.* 2009;158(1-2):171-9.

1167 59. Trager W, and Jensen JB. Human malaria parasites in continuous culture. *Science.*
1168 1976;193(4254):673-5.

60. Lambros C, and Vanderberg JP. Synchronization of Plasmodium falciparum erythrocytic stages in culture. *J Parasitol.* 1979;65(3):418-20.

61. Staalsoe T, Giha HA, Dodoo D, Theander TG, and Hviid L. Detection of antibodies to variant antigens on Plasmodium falciparum-infected erythrocytes by flow cytometry. *Cytometry.* 1999;35(4):329-36.

62. Boyle MJ, Wilson DW, Richards JS, Riglar DT, Tetteh KK, Conway DJ, et al. Isolation of viable Plasmodium falciparum merozoites to define erythrocyte invasion events and advance vaccine and drug development. *Proc Natl Acad Sci U S A.* 2010;107(32):14378-83.

63. Paul F, Roath S, Melville D, Warhurst DC, and Osisanya JO. Separation of malaria-infected erythrocytes from whole blood: use of a selective high-gradient magnetic separation technique. *Lancet.* 1981;2(8237):70-1.

64. Lavinder JJ, Wine Y, Giesecke C, Ippolito GC, Horton AP, Lungu OI, et al. Identification and characterization of the constituent human serum antibodies elicited by vaccination. *Proc Natl Acad Sci U S A.* 2014;111(6):2259-64.

65. Voss WN, Hou YJ, Johnson NV, Delidakis G, Kim JE, Javanmardi K, et al. Prevalent, protective, and convergent IgG recognition of SARS-CoV-2 non-RBD spike epitopes. *Science.* 2021;372(6546):1108-12.

66. Turchaninova MA, Davydov A, Britanova OV, Shugay M, Bikos V, Egorov ES, et al. High-quality full-length immunoglobulin profiling with unique molecular barcoding. *Nat Protoc.* 2016;11(9):1599-616.

67. Edgar RC. Search and clustering orders of magnitude faster than BLAST. *Bioinformatics.* 2010;26(19):2460-1.

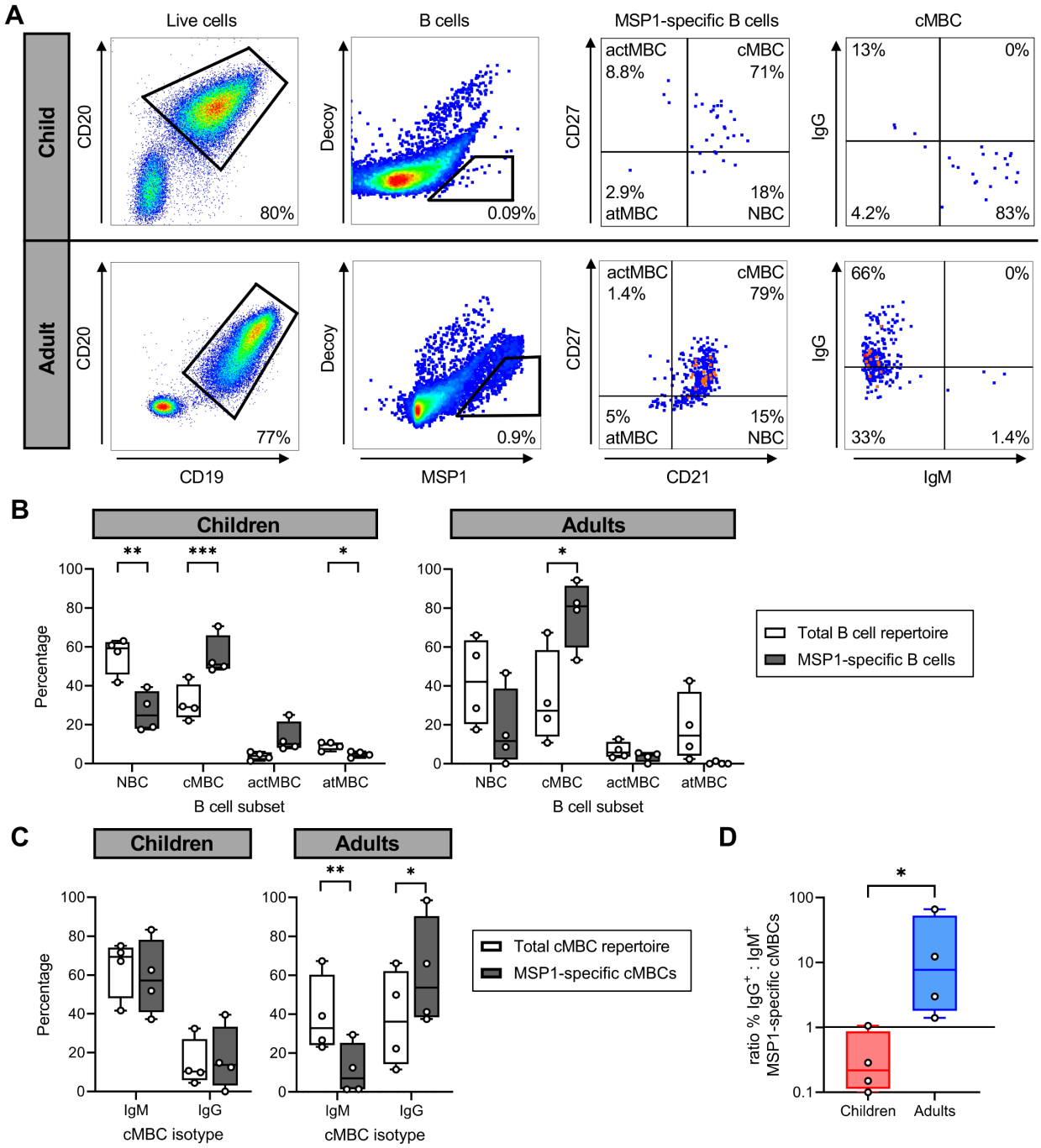


**Figure 1: The isotype of MSP1-specific B cells in malaria-experienced children and adults. A)** Representative flow cytometry gating for the sorting and analysis of MSP1-specific B cells. The four major B cell subsets are defined as follows: naïve B cells (NBC), CD21$^{+}$ CD27$^{-}$; classical memory B cells (cMBC), CD21$^{+}$ CD27$^{+}$; activated

memory B cells (actMBC), $CD21^-$ $CD27^+$; and atypical memory B cells (atMBC), $CD21^-$ $CD27^-$. Data are shown as pseudocolor plots, in which overlapping cells in the plots showing MSP1-specific B cells and cMBCs are shown in orange and red. **B)** Relative abundance of major B cell subsets among the total B cell repertoire and among MSP1-specific B cells in partially immune children (n = 4) and immune adults (n = 4). **C)** The percentage of $IgM^+$ and $IgG^+$ B cells among the total repertoire of cMBCs and among MSP1-specific cMBCs in malaria-experienced children (n = 4) and adults (n = 4). In panels B and C, differences were tested for statistical significance using a paired Student's t-test, even though a non-parametric test would be more appropriate given the small sample size. However, the paired non-parametric alternative (Wilcoxon signed-rank test) does not return a P value lower than 0.13 when using groups of 4. **D)** The ratio of the percentage of $IgG^+$ over $IgM^+$ MSP1-specific cMBCs in malaria-experienced children and adults. A data point with value 0 was plotted at 0.1 for visualization purposes. The difference between groups was tested for statistical significance using a Mann Whitney test. *** $P < 0.001$; ** $P < 0.01$; * $P < 0.05$

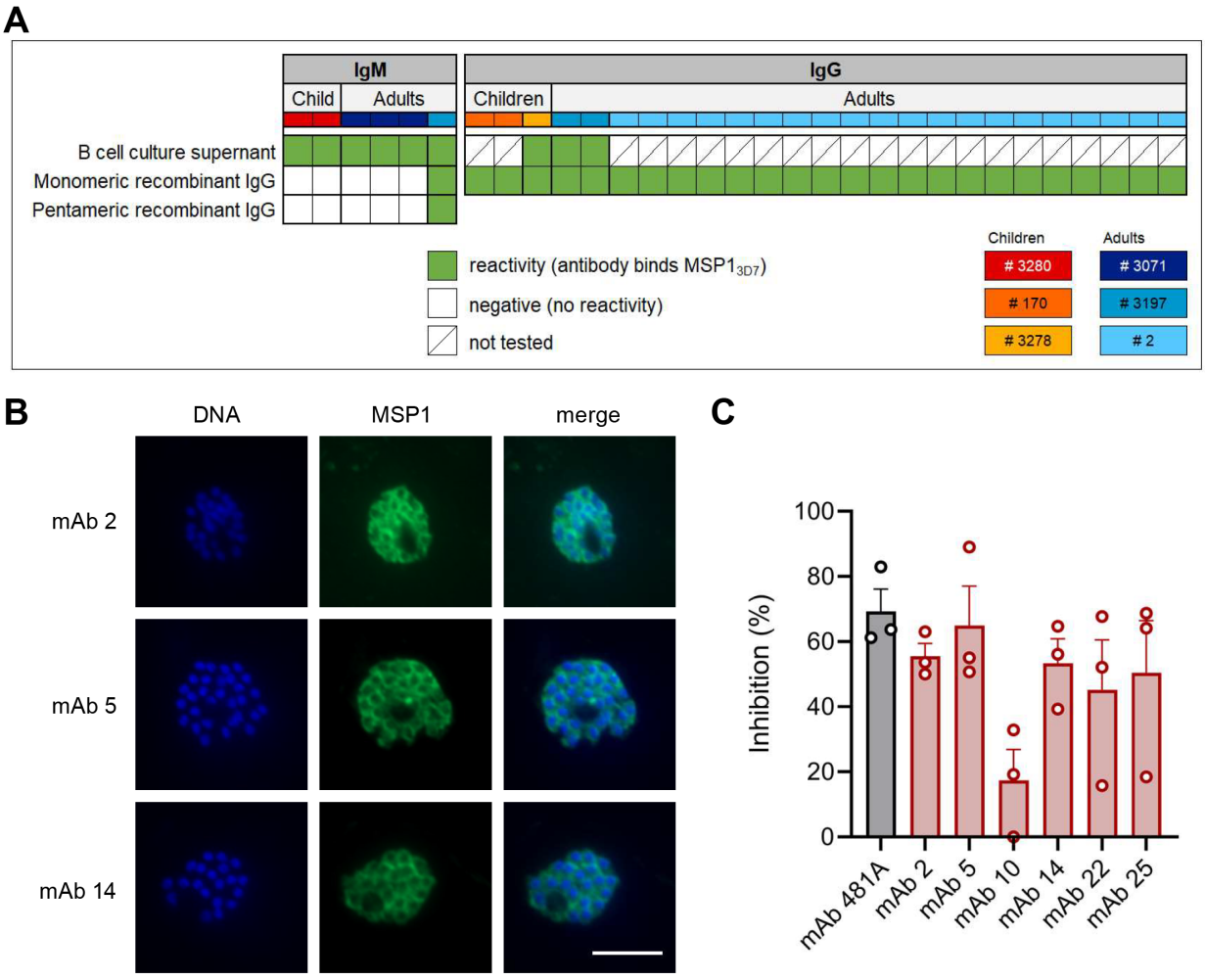


**Figure 2: $MSP1_{3D7}$ reactivity and growth inhibitory activity of anti-MSP1 monoclonal antibodies isolated from memory B cells. A)** $MSP1_{3D7}$ reactivity of supernatants of clonal MBC cultures or mAbs obtained from MBCs (recombinant IgG) determined by ELISA or Luminex assay. The donor from whom mAbs were isolated is color-coded in the top row. Recombinant mAbs that were derived from $IgM^+$ MBCs were tested as both monomeric and pentaimeric recombinant IgG. **B)** Immunofluorescence imaging of segmented schizonts using three select mAbs isolated from MBCs of adult donor 2. At this stage, parasites consist of 16 – 32 merozoites, each with its own nucleus, and express MSP1 on the parasite cell surface. Representative images of two

1224 experiments are shown. Scale bar is 5 μm. **C)** *P. falciparum* growth inhibition by six
1225 select mAbs isolated from adult donor 2. Inhibition was calculated relative to a negative
1226 control. Results shown are the average + SEM from three independent experiments.
1227 mAb 481A served as a positive control.
1228

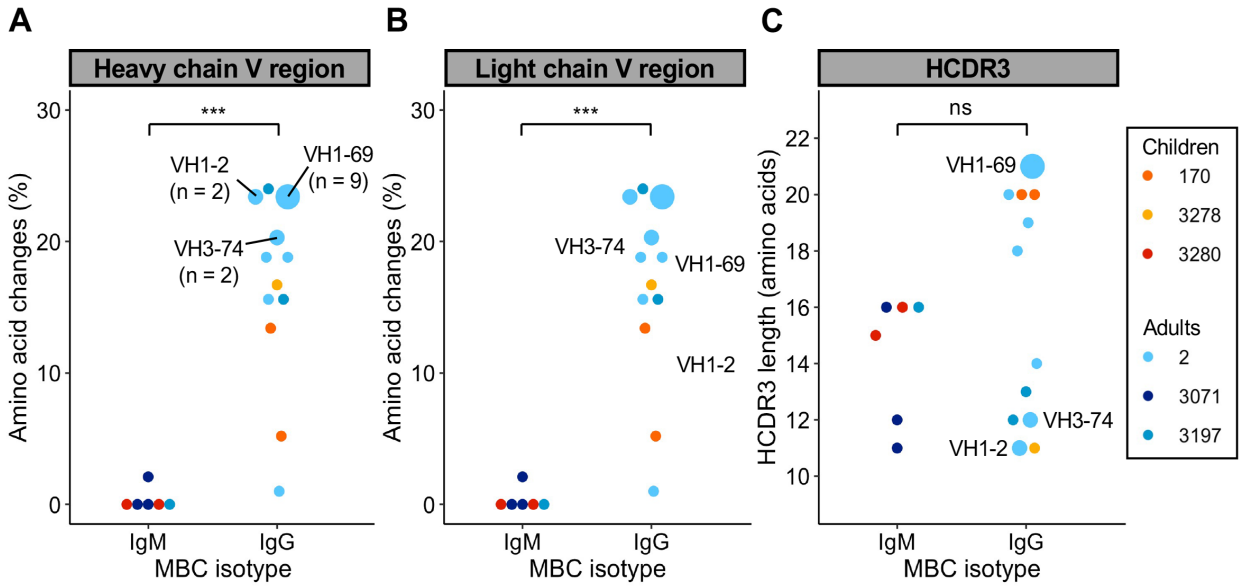


1229

1230 **Figure 3: Sequence analysis of the variable heavy and light chains of MSP1-**

1231 **specific memory B cells. A-B)** Percentage of amino acid changes in the V gene

1232 segments of the heavy chain (A) and light chain (B) variable regions. **C)** Length of

1233 HCDR3s. In all graphs, sequences from expanded clonal lineages were grouped. The

1234 VH gene usage and size of expanded clonal lineages are indicated. Differences

1235 between $IgM^+$ (n = 6) and $IgG^+$ (n = 13 for heavy chains / n = 14 for light chains) MBC

1236 lineages were evaluated for statistical significance using a Mann Whitney test.

1237

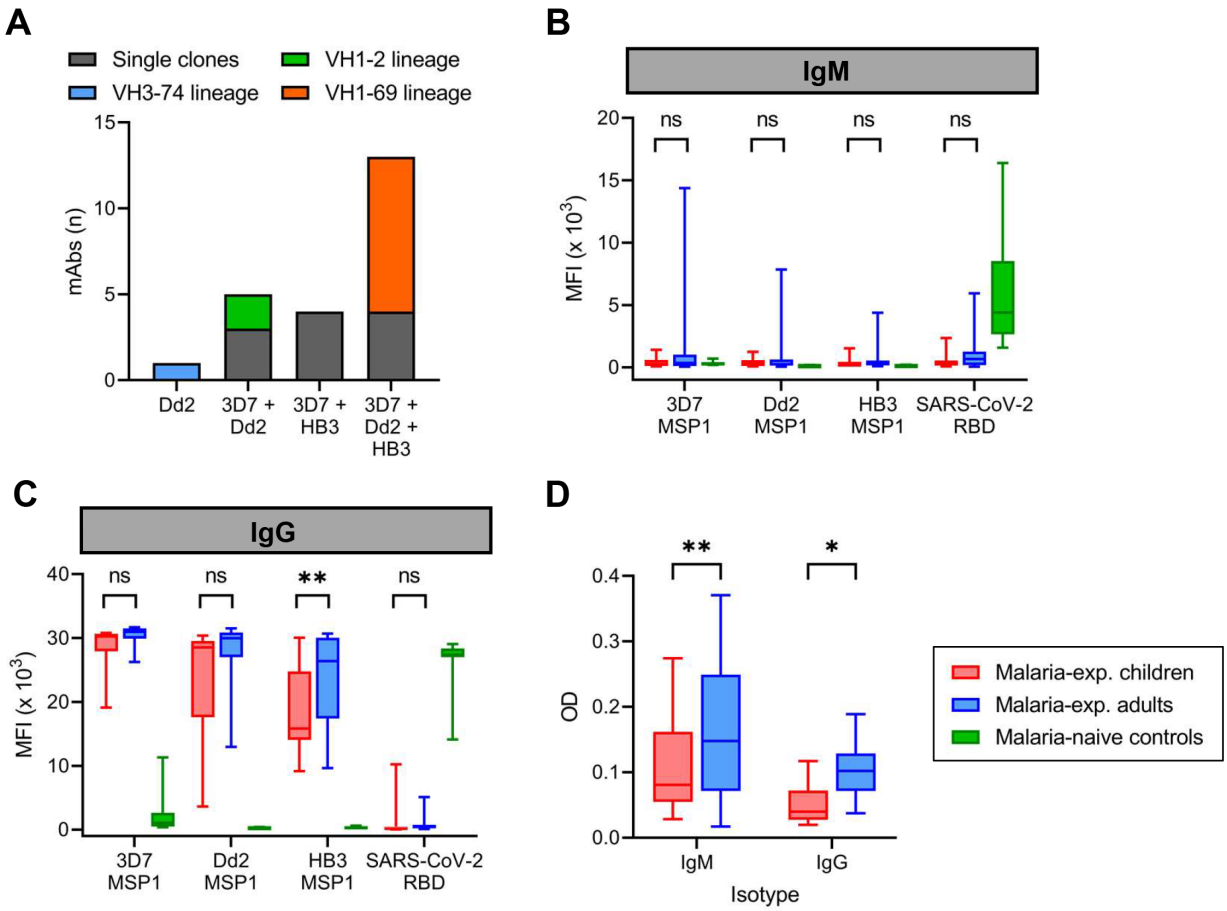


**Figure 4: Reactivity of monoclonal antibodies and plasma IgM and IgG against different strains of *P. falciparum.* A)** The number of anti-MSP1 recombinant monoclonal antibodies (mAbs) with reactivity against recombinant MSP1 of three different *P. falciparum* strains in a Luminex assay. Each mAb is shown as a stacked block and is color-coded based on whether it was a single clone or derived from an expanded clonal B cell lineages. The VH3-74 lineage consisted of two MBCs, of which we were unable to retrieve the light chain for the second mAb. For this reason, only a single mAb of this lineage was tested here. **B-C)** Reactivity of plasma IgM (B) and IgG (C) from malaria-experienced children (n = 18) and adults (n = 24), and malaria-naïve recovered US COVID-19 patients (control; n = 10) against recombinant MSP1 of *P.*

*falciparum* strains 3D7, Dd2, and HB3, as well as SARS-CoV-2 receptor binding domain (RBD), as determined by Luminex assay. Values shown are mean fluorescence intensity (MFI). **D)** Reactivity of plasma IgM and IgG from malaria-experienced children (n = 18) and adults (n = 24) against whole merozoites by ELISA. Values shown are optical densities after subtraction of background values obtained using pooled unexposed plasma from US donors. Data shown in panels B – D were tested for statistical significance using a two-way repeated measures ANOVA, followed by comparisons between children and adults using Šídák's post-hoc test, corrected for multiple comparisons. ** $P < 0.01$; * $P < 0.05$

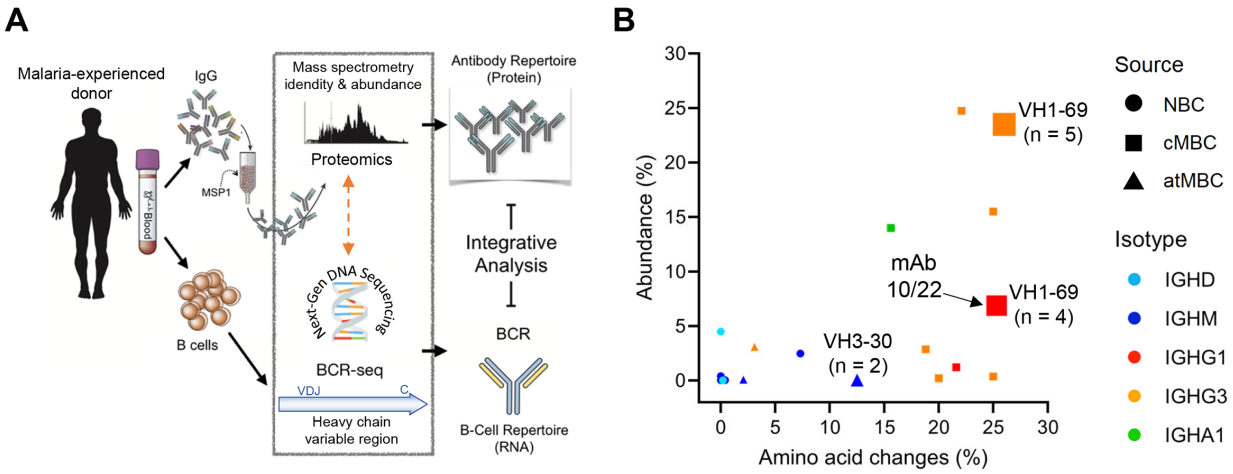


**Figure 5: Analysis of the repertoire of anti-MSP1$_{19}$ IgG in the plasma of a malaria-experienced adult. A)** Schematic overview of the experimental pipeline. **B)** The percentage amino acid changes in the V gene segment of the heavy chain variable region (as determined by B cell receptor sequencing; X axis) plotted against the abundance of the corresponding IgG in plasma (Y axis). The size of the data points indicates the number of clonal sequences found in the B cell receptor sequencing (BCR-seq) data set, as a measure of the size of the clonal B cell lineage. The three lineages that were expanded in the BCR-seq data set are indicated with a number, that represents the number of clonal sequences identified by BCR-seq. The shape of the data point shows the B cell subset among which the sequence was found (NBC, naïve B cell; cMBC, classical memory B cell; atMBC, atypical memory B cell), while the color indicates the B cell isotype. The data point corresponding to mAb10 and mAb22 (isolated from MSP1-specific B cells) is indicated with an arrow.

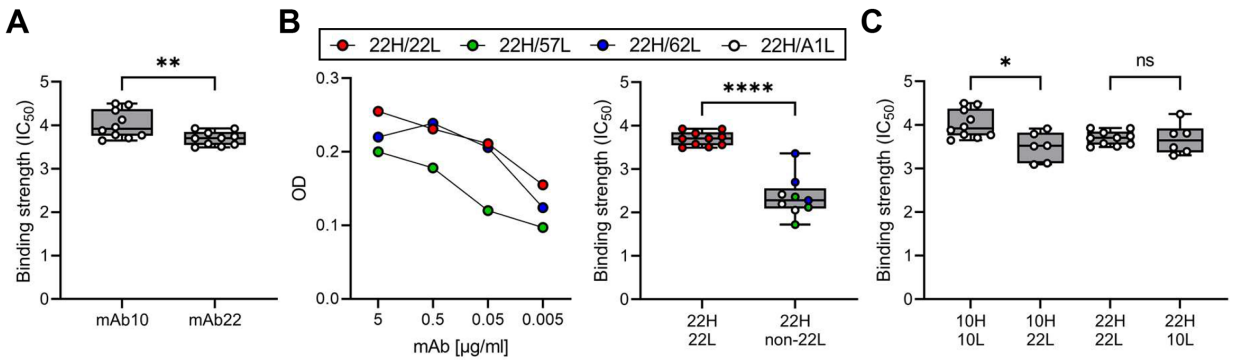


**Figure 6: Binding affinity of mAb10 and mAb22 to $MSP1_{3D7}$. A)** The binding strength of mAb10 and mAb22 as determined by chaotropic ELISA. Binding strength ($IC_{50}$) is defined as the concentration of urea that results in loss of 50% of mAb binding. A total of 10 replicates from three independent experiments are shown. Differences were tested for statistical significance using the Wilcoxon matched-pairs signed rank test, with pairs were defined as antibodies analyzed on the same plate. **B)** The binding of mAb22 and antibodies that consisted of the heavy chain of mAb22 and a light chain of an unrelated, non-MSP1-reactive antibody to $MSP1_{3D7}$ by regular ELISA (left) and chaotropic ELISA (right). Differences in binding strength between replicates of mAb22 (n = 10) and chimeric antibodies (n = 9, three replicates for each of three unrelated light chains that were combined for analysis) were tested for statistical significance using the Mann Whitney test. **C)** The binding strength of mAb10 and mAb22 (n = 10 replicates each) expressed with their own light chains or chimeric mAbs in which the light chains were swapped (n = 6 replicates each). In all panels, data points are the average of three technical replicates. Differences between antibodies with the same heavy chain but a different light chain were tested for statistical significance using a Kruskal-Wallis test, followed by comparisons between select groups using Dunn's post-hoc test, corrected for multiple comparisons. **** $P < 0.0001$; ** $P < 0.01$; * $P < 0.05$